

**CZECH TECHNICAL UNIVERSITY IN PRAGUE
FACULTY OF CIVIL ENGINEERING**

DEPARTMENT OF STEEL AND TIMBER STRUCTURES



&

**TECNOLÓGICO DE COSTA RICA
ESCUELA DE INGENIERÍA EN CONSTRUCCIÓN**

TEC | Tecnológico
de Costa Rica

**THE EFFECT OF OPENINGS ON STRESS
DISTRIBUTION IN GLASS BEAMS**

MASTER'S THESIS

Bc. Martin Lavko

SUPERVISORS:

**Ing. Zdeněk Sokol, Ph.D.
Ing. Giannina Ortíz Quesada**

2017/2018



ČESKÉ VYSOKÉ UČENÍ TECHNICKÉ V PRAZE

Fakulta stavební
Tháškova 7, 166 29 Praha 6

ZADÁNÍ DIPLOMOVÉ PRÁCE

I. OSOBNÍ A STUDIJNÍ ÚDAJE

Příjmení: Lavko	Jméno: Martin	Osobní číslo: 410828
Zadávací katedra: Katedra ocelových a dřevěných konstrukcí (K134)		
Studijní program: Magisterský		
Studijní obor: Konstrukce pozemních staveb		

II. ÚDAJE K DIPLOMOVÉ PRÁCI

Název diplomové práce: Vliv otvorů na rozložení napětí na skleněném nosníku	
Název diplomové práce anglicky: Effect of openings on stress distribution in glass beam	
Pokyny pro vypracování: Vytvoření numerického modelu skleněného nosníku s otvory a jeho ověření na experimenty, vypracování numerické studie zaměřené na velikost a polohu otvorů na nosníku	
Seznam doporučené literatury:	
Jméno vedoucího diplomové práce: Ing. Zdeněk Sokol, Ph.D.	
Datum zadání diplomové práce: 19.2.2018	Termín odevzdání diplomové práce: 20.5.2018 <i>Údaj uveďte v souladu s datem v časovém plánu příslušného ak. roku</i>
Podpis vedoucího práce	Podpis vedoucího katedry

III. PŘEVZETÍ ZADÁNÍ

Beru na vědomí, že jsem povinen vypracovat diplomovou práci samostatně, bez cizí pomoci, s výjimkou poskytnutých konzultací. Seznam použité literatury, jiných pramenů a jmen konzultantů je nutné uvést v diplomové práci a při citování postupovat v souladu s metodickou příručkou ČVUT „Jak psát vysokoškolské závěrečné práce“ a metodickým pokynem ČVUT „O dodržování etických principů při přípravě vysokoškolských závěrečných prací“.

22.02.2018	Podpis studenta(ky)
Datum převzetí zadání	

Statutory declaration

I hereby declare that the master's thesis entitled "The effect of openings on stress distribution in glass beams" submitted to Czech Technical University in Prague was written by myself under the guidance of Ing. Zdeněk Sokol, Ph.D and Ing. Giannina Ortíz Quesada. I have stated all the resources used to elaborate this thesis in conformity with the Methodical guide for ethical development of university final thesis.

15th May 2018

.....
Martin Lavko

Aknowledgements

First of all I am very grateful to my supervisors Giannina Ortíz Quesada and Zdeněk Sokol for their guidance, motivating discussion and helpful advices during my study. I appreciate their effort on international cooperation and coordination of the present thesis.

I would also like to give my thanks to Martina Eliášová for her encouraging help with experiments and for introducing me into theory of glass load bearing structures.

Also I would like to show my appreciation to the company OGB s.r.o. for providing me with samples from their production and to Michal for creating supporting steel structures necessary for the experiments.

Last but not least, thanks belong to my family and dearest, as I appreciate their support and patience during my studies.

Abstract

Presented master's thesis describes the behaviour of simply supported single ply glass beam with discontinuities in its geometry. Discontinuity is introduced by four openings symmetrically placed over the beam. This type of simplified structure represents cut out of real constructions where similar glass components are used as primary load bearing structures supporting glazings of roofs or decks of pedestrian bridges. The main focus of this thesis is in research of stress distribution around openings and how different diameter of a hole and its placement with respect to the edges of beam influence stresses in its close proximity. As Eurocode standards for glass structures are still not codified and most of the nowadays literature only provide suggested diameters of holes and their distance to the edge based on the thickness of the glass pane this thesis will provide the future designers of glass load bearing structures with closer look at stress distribution around mentioned area. In order to bring those informations to theirs seekers, both experimental analysis and numerical analysis together with parametric study were used.

Key words: glass, glass load bearing structures, beams, holes, stress distribution, heat-strengthened, one ply beam, simply supported

Abstrakt

Predkladaná diplomová práca sa zaoberá pôsobením prostého nosníka z jednovrstvého skla s diskontinuitami v jeho geometrii. Diskontinuita je zavedená štyrmi otvormi symetricky umiestnenými na nosníku. Tento typ zjednodušenej konštrukcie predstavuje výrez z reálnej konštrukcie, kde sú obdobné sklenené komponenty použité ako primárne nosné konštrukcie podporujúce zasklenie striech alebo pochôdznych častí mostov pre peších. Hlavným zameraním tejto práce je skúmanie rozloženia napätia okolo otvorov a vplyvu rozdielneho priemeru otvorov a ich umiestnenia na nosníku vzhľadom na vzniknuté napätie v ich tesnej blízkosti. Vzhľadom na to, že Eurokódové normy pre sklenené konštrukcie ešte nie sú kodifikované a väčšina súčasnej literatúry poskytuje iba doporučené priemery otvorov a ich vzdialenosť od okraja na základe hrúbky sklenenej tabule, táto práca poskytne budúcim dizajnérom sklenených nosných konštrukcií bližšie oboznámenie sa s priebehom napätia v uvedenej oblasti. K dosiahnutiu a poskytnutiu týchto informácií budúcim dizajnérom nosných konštrukcií zo skla sa použila ako aj experimentálna analýza, tak numerická analýza spolu s parametrickou štúdiou.

Kľúčové slová: sklo, nosné konštrukcie zo skla, nosníky, otvory, rozloženie napätia, tepelne spevnené sklo, jednovrstvé sklo, prostý nosník

Contents

1	Introduction	7
2	Glass as a building material	8
2.1	Making of glass	9
2.2	Mechanical properties of glass.....	10
2.3	Types of glass by raw materials content	12
2.4	Types of glass by method of production	14
2.4.1	Float glass	14
2.4.2	Heat-strengthened glass	15
2.4.3	Tempered glass	15
2.4.4	Chemically strengthened glass.....	16
2.4.5	Laminated glass.....	17
2.5	Coating the panes.....	20
2.5.1	On-line coatings.....	20
2.5.2	Off-line coatings	20
2.6	Cutting, drilling and grinding	21
2.7	Glass structures connections.....	22
2.7.1	Glass load bearing structures.....	23
2.7.2	Types of connections used in buildings.....	24
3	The aim of master's thesis	31
4	Experimental analysis	32
4.1	Testing equipment.....	32
4.1.1	MTS QTest 100	32
4.1.2	Rod-type borehole extensometer.....	33
4.1.3	Dewetron DEWE-5000.....	33
4.1.4	The "2 x IPE table"	34
4.1.5	Lateral buckling restraint	35
4.1.6	The loading cell.....	35
4.2	Geometry of the specimens	36
4.3	Testing procedure.....	38
4.3.1	Four point flexural test.....	38

4.3.2	Strain gauges placement	39
4.3.3	Measurement of vertical deflection.....	41
4.3.4	Failure expectations	42
4.4	Loading of the specimens	43
4.5	Results.....	45
4.6	Comparison of specimens and conclusion	49
5	Numerical analysis	52
5.1	FEA and meshed model	52
5.2	Numerical model	54
5.2.1	Input data	54
5.2.2	The mesh	56
5.2.3	Boundary conditions and load	57
5.2.4	Results	57
5.3	Parametric study.....	60
5.3.1	Variable position	60
5.3.2	Variable radius.....	62
6	Conclusion.....	65
6.1	Future extensions	66
7	Bibliography	67

List of figures

Figure 2.1: All-glass staircase surrounded by glass glazing with glass fins [6]	8
Figure 2.2: Scheme of a glass making process [8]	10
Figure 2.3: Percentage distribution of transmitted, reflected and absorbed light [1]	10
Figure 2.4: Comparison of stress-strain diagrams of steel and glass [1]	11
Figure 2.5: Obsidian from Turrialba Volcano, Costa Rica	13
Figure 2.6: Stress distribution in tempered glass cross-section [4]	16
Figure 2.7: Comparison of stress distribution in cross-sections of tempered and chemically strengthened glass [2]	17
Figure 2.8: Behaviour of laminated glass according to duration of load [2]	18
Figure 2.9: Photovoltaic cells located in the interlayer of laminated glass [1]	19
Figure 2.10: Recommended positioning of holes (conservative approach intended for guidance only) [1]	22
Figure 2.11: Types of supports of glass slabs [4]	25
Figure 2.12: Standard bolt connection – shear bolt [4]	25
Figure 2.13: Simple countersunk-head bolt [4]	26
Figure 2.14: Bearing bolt connection with steel splices [4]	27
Figure 2.15: Bolted connection with stud assembly [4]	28
Figure 2.16: Spider connection [4]	29
Figure 2.17: Stress distribution in connection made with hard adhesive [4]	30
Figure 2.18: Stress distribution in connection made with thick elastic adhesive [4]	30
Figure 4.1: MTS QTests 100	32
Figure 4.2: Rod-type borehole extensometer with magnetic holder	33
Figure 4.3: Dewetron DEWE-5000 with DEWEsoft software [18]	34
Figure 4.4: The table with cylindrical supports	34
Figure 4.5: Lateral buckling restraint (distance in mm)	35
Figure 4.6: The loading cell (distance in mm)	36
Figure 4.7: Drawing from the providing documentation of the glass beams	37
Figure 4.8: Scheme of the loading assembly (distances in mm)	37
Figure 4.9: The loading assembly ready for specimen insertion	38
Figure 4.10: Moment distribution in four point flexural test	39
Figure 4.11: Measured values during the tests	39
Figure 4.12: Location and orientation of strain gauges (distances in mm)	40
Figure 4.13: 2 rod extensometers placed on a L-shaped steel component	41
Figure 4.14: Rod extensometer above the support and noticeable pressing of the beam to polyamide	42
Figure 4.15: Specimen N04 before testing	43
Figure 4.16: Storage of specimen N03 with glued strain gauges	45
Figure 4.17: Specimen N01 ready for loading	45
Figure 4.18: The crack pattern of the tested beam	47
Figure 4.19: Point of the initial crack (marked red)	48
Figure 5.1: Element SOLID185 [20]	53

Figure 5.2: Element SOLID95 [20]	53
Figure 5.3: Geometry of used model	54
Figure 5.4: Finite elements mesh generated in the Mechanical interface	56
Figure 5.5: Static scheme of used model	57
Figure 5.6: Vertical deflection of numerical model.....	58
Figure 5.7: Stress distribution on the modelled beam in MPa	59
Figure 5.8: Maximum stress at the edge of lower opening in MPa	60
Figure 5.9: Distances "a" and "b"	61

List of tables

Table 2.1: Material properties of glass [5]	12
Table 2.2: Optical properties of various solar control coatings [1].....	21
Table 4.1: Maximum force - deflection reached for each specimen	50
Table 5.1: Material properties of Heat-strengthened glass used for model	55
Table 5.2: Material properties of Structural steel used for model	55
Table 5.3: Input and output parametric quantities for variable position of opening.....	61
Table 5.4: Input and output parametric quantities for variable radius of opening.....	63

List of charts

Graph 4.1: Force - deflection diagram, specimen N01	46
Graph 4.2: Force - deflection diagram, specimen N02	47
Graph 4.3: Force - deflection diagram, specimen N03	49
Graph 4.4: Comparison of all 3 specimens.....	51
Graph 5.1: Comparison of ideal beam and numerical model	58
Graph 5.2: Correlation between the axial distance between the openings and stiffness	61
Graph 5.3: Correlation between the axial distance between the openings and maximum principal stress at the edge of hole	62
Graph 5.4: Correlation between the area of the opening and stiffness.....	63
Graph 5.5: Correlation between the radius of the opening and maximum principal stress at the edge of hole	64
Graph 5.6: Correlation between the radius of the opening and maximum principal stress at the edge of hole after subtracting the effect of different edge position alongside the height of beam	64

List of symbols

E – Young's modulus

G – Shear modulus

δ – Deflection

σ - Stress

ν – Poison's ratio

F – Force

K – Stiffness

r – Radius

A – Hole edge to beam edge distance

S – Thickness of a glass pane

D – Diameter of a hole

1 Introduction

Among traditional materials used in constructions such as concrete, steel, timber and masonry, more often materials like glass emerged in last decades. Glass, substance used for centuries only as a fill of openings serving for bringing light into a building and creating transparent barrier between exterior and interior is nowadays, thanks to its unique properties used for constructions like slabs, beams and columns. Wide spread of using glass is brought by modern architecture and progressive architects who are not afraid of designing subtle and transparent structures. Glass as a load bearing material has irreplaceable place in Building construction bussines of 21th century, where is used for glazing of fasades, bridges, ceilings and staircases. When used as a load bearing structure it not only transfers self-weight to other load bearing structures, but actively tranfers loads like wind, snow or forces acting on structure during fire, to foundations and then to soil.

Glass, compared to other common materials used in building industry, has a unique mechanical and optical properties which open whole new range of construction details where it can be applied. Its high level of flatness allow engineers to design slender columns, beams and slabs, which also fulfil strict strength, reliability and safety requirements for buildings. Relative to timber, glass is isothropic, which means, it has the same material properties in each point of a specimen. Moreover, it has equal tensile and compressive strength and strength of tempered glass exceeds compressive strength of commonly used concretes. But the characteristic which expels it between the most favourit materials among modern architects is transparency. This feature can't be found in any other substance applied in constructions. On the other hand, glass is fragile and furthermore one layer glass structures do not have any residual strength which limits utilization of it in load bearing structures.

The aim of this work is to better understand stress distribution in glass beams with two or more vertical openings and help designers by providing them with infotmation about stress distribution around holes depending on mutual distances between holes themself and an edge of a beam validated by experimental and numerical analysis.

2 Glass as a building material

Natural glass can be found in form of a solid lava, also known as a volcanic glass (obsidian). It can be created by impact events as well, such as strike of meteorite (tektites), lightning strike (fulgurite) or by burning of coal. First use of glass, the natural ones such as obsidian is dated 5000 years ago. It was found in forms of jewellery and basic tools.

Among the first modern glass constructions we can include English greenhouses built in the early 19th century. In order to achieve the greatest possible heat gain, the constructors gradually reduced the ratio of the metal used to the glass until they developed a loosely-arched roof made of a large number of smaller-sized glass panes. Also, these glass panes attached to the sealant ensure the reinforcement of the whole structure.[1]



Figure 2.1: All-glass staircase surrounded by glass glazing with glass fins [6]

Nowadays, with the development of architecture, glass in constructions as a load-bearing element and all-glass structures are becoming more and more common. Up to 70% of the total production of flat glass is used in new buildings or renovations of building envelopes [1]. A large part of glass made for application in buildings is used for large-scale facades, atriums or railing structures, but more and more often glass finds its use in glass beams, columns and staircases.

2.1 Making of glass

The basis for making glass is a mixture of raw materials. The main raw material for glass production is glass sand containing 60-80% silicon dioxide. Other ingredients of conventional glass are calcium oxide, sodium oxide and potassium oxide. These oxides are supplied to the strain in the form of minerals (limestone) or chemically prepared raw materials (soda). A certain proportion in the production of new glass consists of crushed waste glass (glass fragments). Glass sand in the required quality does not occur naturally, so it is necessary to modify it, by grinding, washing, sorting and reducing the content of coloring oxides (Fe_2O_3) in the desired high glass quality. [7]

The technological process of glass production is divided into 4 parts as follows:

- Preparation of the raw materials and additives - Adjusted, milled and dried raw materials are mixed and homogenized in the desired ratio in the mixing devices. [7]
- Melting of glass - The melting process takes place in glass melting furnaces and is divided into 3 main phases: own melting, chilling and homogenization, cooling for shaping. When melting, the temperature is 1400-1600 ° C. [7]
- Glass floating - The molten glass is gradually cast into a tin bath where, due to different glass and tin densities, it floats and produces a level of constant thickness. Tin is used because of its high temperature range, where it remains in the liquid state. Subsequently, the glass is cooled and rolled. The thickness of the glass depends on the speed of the rollers. [7,2]
- Annealing - The glass is cooled in special annealing lehr in a temperature range of 700 - 400 ° C. This controlled cooling removes internal tension. After annealing, the glass is proceeded to cutting section. After cutting it to required proportions surface is treated (grinding, polishing). [7]

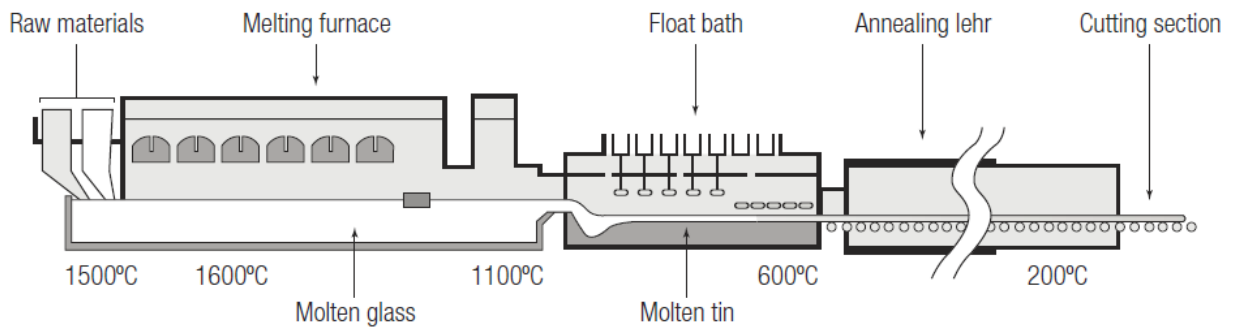


Figure 2.2: Scheme of a glass making process [8]

2.2 Mechanical properties of glass

Because of its specific mechanical properties, glass has an indispensable place between building materials. It is an amorphous material (it does not have a crystalline structure) and is isotropic (it has the same properties in all directions). The main advantages of glass include its transparency. Transparency is the ability of the material to release a visible component of the sun's radiation, in the case of glass, part of the radiation is absorbed, the part is reflected and part is transmitted (Fig. 2.3).

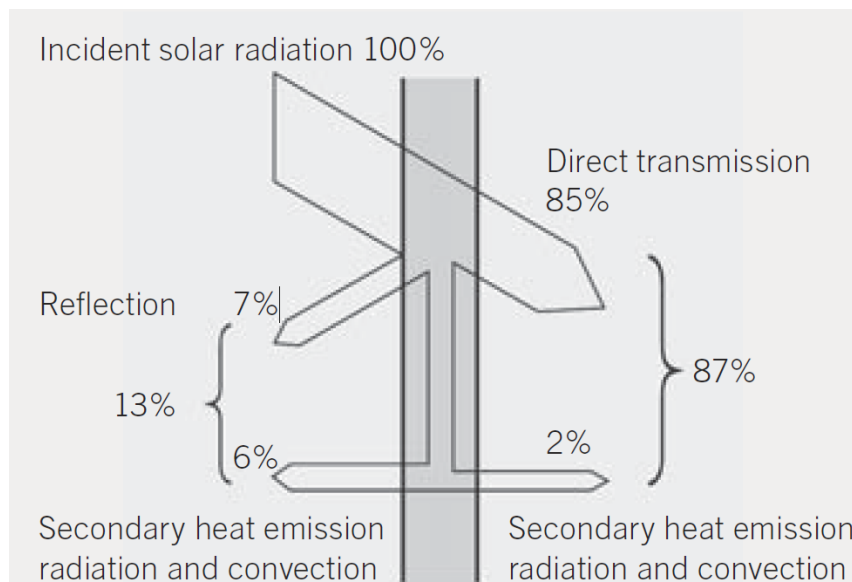


Figure 2.3: Percentage distribution of transmitted, reflected and absorbed light [1]

The fact that glass is transparent has considerably influenced its use in the past centuries, where the building industry used it essentially to illuminate interiors and enhance

the lightning environment and people's comfort. Gradually, as the quality of glass making technology improved, the flatness, strength and other characteristics of the glass increased, which allowed a wider range of use of this material in constructions.

A critical disadvantage of glass compared to conventional building materials such as steel, concrete or timber remains in its fragility (*Figure 2.4*). When the maximum load capacity of the single-ply glass plate of float glass is exceeded, the crack spreads from the point of origin to edges and the collapse is almost instantaneous. When broken, sharp shards of different shapes and sizes are created. Increase in residual strength can be reached by laminating. The process of lamination consists of connecting 2 or more plies with thin foil which prevents the shards from dropping out of plane. Those shards are jammed to each other and a broken specimen can show post-breakage strength. Danger is in slitting the thin foil with shards and even though glass was laminated, it can result in the pieces falling out of construction.

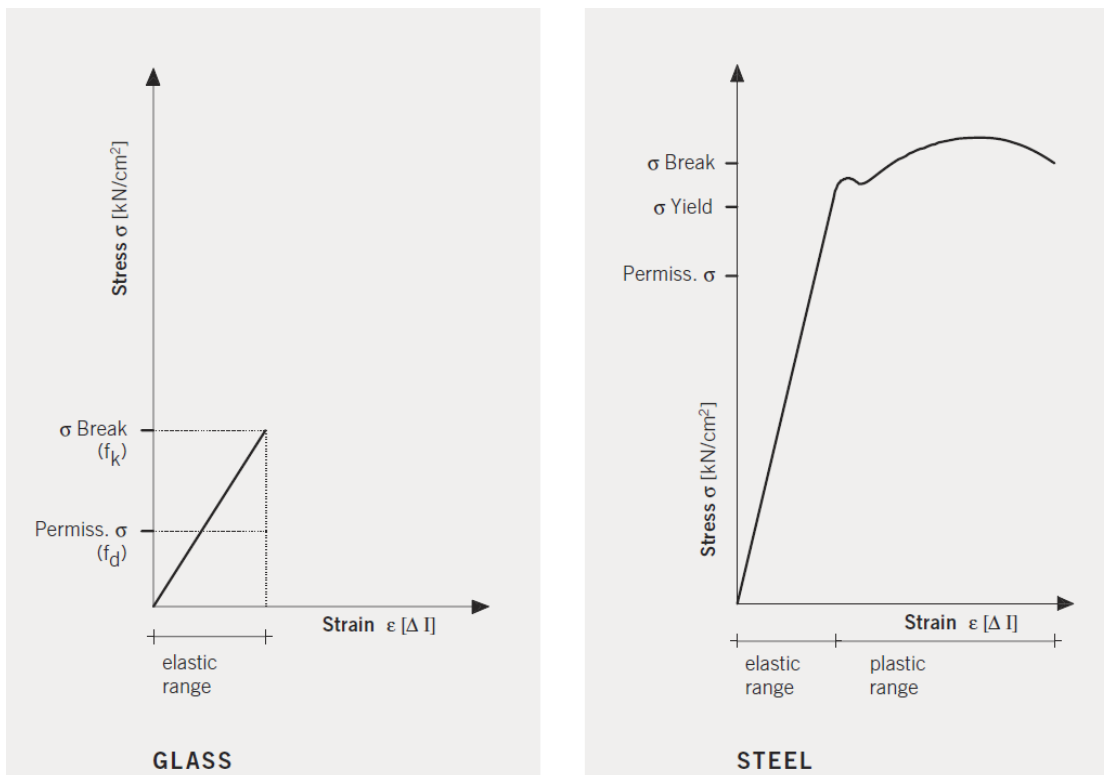


Figure 2.4: Comparison of stress-strain diagrams of steel and glass [1]

Some of the float glass characteristics that are relevant to the design of the glass structures are shown in the following table.

Property	Value	Units
Density	2 520	Kg · m ⁻³
Tensile strength	20 – 100	MPa
Compression strength	400 – 900	MPa
Modulus of elasticity E	70 – 74	GPa
Shear modulus G	20 – 30	GPa
Poisson's ratio	0,22 – 0,25	-
Thermal expansion factor	8 x 10 ⁻⁶ – 9 x 10 ⁻⁶	K ⁻¹

Table 2.1: Material properties of glass [5]

2.3 Types of glass by raw materials content

In general, glass can be divided into natural glass (obsidian) and artificial glasses produced by melting glass sand and additives (*Chapter 2.1*). In the constructions, only artificially made glass is used. The ingredients and the method of production vary, depending on the desired properties of the glass element placed in structures and on the external influences which will affect it throughout the life-cycle. Depending on a type and amount of ingredients we recognize the following types of glass:

- Fused quartz – formed by melting a pure crystal or venous cremene, a substantial amount of SiO₂ [7].
- “Water” glass – produced by melting silica sand with sodium oxide Na₂O (3,1 – 3,3%), in the past used as an additive for fire-resistant sprayings and paintings [7].

- Soda-lime-silica glass – the most common type of glass, used for windows, composition: SiO_2 (70 – 73,5%), Al_2O_3 (0,6 – 2,0%), CaO (6 – 11%), MgO (1,5 – 4,5%), Na_2O (13 – 15%), colored glass can be made by adding coloring metal oxides (Fe_2O_3 , MnO)[7].
- Crystal glass – a high-quality, colorless type of glass with high gloss and high light transmittance [7].
- Sodium borosilicate glass – glass having a linear coefficient of thermal expansion less than $5 \cdot 10^{-6} \text{ K}^{-1}$, it contains B_2O_3 (8% and more) [7].
- Low-alkaline glass – low content of K_2O and Na_2O , used in the pharmaceutical industry [7].



Figure 2.5: Obsidian from Turrialba Volcano, Costa Rica

2.4 Types of glass by method of production

At present, glass production is focused on the production of float glass, which is the most used type in constructions. However, the strength of this type of glass is insufficient in the exposed parts of structures. Therefore, glass is further processed by tempering, chemical strengthening or laminating. According to the production method, we distinguish types of glass as follows [2]:

- Float glass
- Heat-strengthened glass
- Tempered glass
- Chemically strengthened glass
- Laminated glass

2.4.1 Float glass

Float glass is produced by the floating process also known as Pilkington process invented in 1952 which is currently fully automated [9]. The basic raw materials for making this type of glass are siliceous sands, soda, limestone and sodium sulphate. These additives are mixed with the crushed glass and heated to a temperature of 1500 ° C until melted. The molten glass is poured into a tin bath on which it floats and creates a glass ribbon of uniform thickness. Thickness of glass can be regulated by the stretching effect of the conveyers. At the end of the production process the glass is slowly cooled and cut to the so-called JUMBO dimension of 3.21 x 6.0 m. Then treatment of edges and adjusting the surfaces is made according to the needs of an end-user. The total length of the glass production line is approximately 500 m. Typical glass thicknesses are 4, 5, 6, 8, 10, 12, 15, 19 mm. Under current manufacturing conditions it is possible to make sheets up to a thickness of 25 mm and a length of 12 m to 14 m [2].

The glass is characterized by its elastic deformation and brittle fracture, which occurs as soon as the maximum load capacity of the glass element is reached. When broken, the float glass structure is displaced from its supports in relatively large and sharp shards that may

endanger the users. Therefore, the use of classical float glass in construction is considerably limited.

One of the possibilities of preventing glass from dropping out of supports and increasing its carrying capacity even after being broken is wired glass. However, these wires are the source of cracks that reduce its load bearing capacity. The bending strength of the wired glass is approximately half of the bending strength of the float glass.

2.4.2 Heat-strengthened glass

The base of heat-strengthened glass is float glass, which is heated to 620 ° C and subsequently rapidly cooled. In this process of production, the cold air first cools the surfaces of the glass which solidifies. The core of the glass pane is gradually cooled, which shrinks due to temperature contraction during cooling and thus leads to prestressing both surfaces [2]. The prestressing load embedded into heat-strengthened glass specimen ranges from 24 to 52 MPa according to EN 1863.

When broken, shards of heat-strengthened glass have similar shape to the ones of float glass. They are sharp and commonly bigger with irregular shapes. Prior to thermal consolidation, the glass must be cut to the required size, including drilling holes and the edges treatment, as it would break if those processes would be done after strengthening [9].

2.4.3 Tempered glass

The process of glass tempering is similar to the process of producing heat-strengthened glass. The float glass panel is heated to the same temperature as in the previous case, but the subsequent cooling is more significant, leading to higher values of prestress in the surfaces. For this type of glass, the prestressing values range from 80MPa to 150MPa [2]. Cutting, drilling holes and edging must be done before the heat treatment.

This type of glass is normally produced in a horizontal position up to the thickness of 19 mm. Failure occurs suddenly over the entire glass surface due to the loss of energy [9]. Shards are small in size, so this type of glass is more suitable for use in spaces with active movement of persons who could be hit by falling shards.

The disadvantage of tempered glass is the possibility of self-spontaneous burst, which is caused by an increased volume of nickel sulphide (NiS). The NiS compound during the sealing process changes the crystal lattice and the coefficient of thermal expansion is then greater than the coefficient of thermal expansion of the glass [9]. This phenomenon usually occurs in the first five years of glass life [2]. To prevent this breakdown before installing the glass into the structure, a destructive thermal shock test (Heat-Soak test) is performed. The test is performed by heating the glass to 300 ° C for eight hours. Damaged glass is excluded [9]. Another disadvantage of tempered glass is the imperfection caused by the movement of the glass sheet on the rollers during manufacture. Deformation has the shape of a sinusoid.

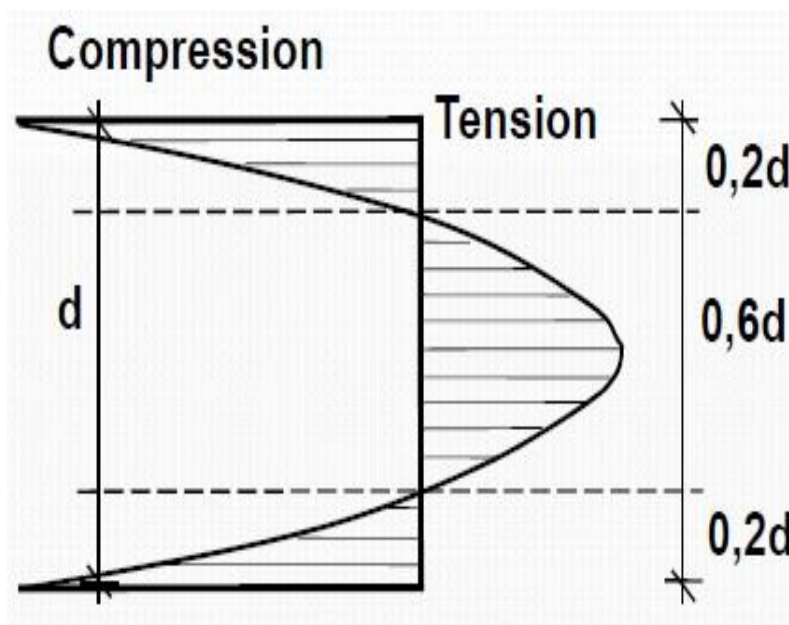


Figure 2.6: Stress distribution in tempered glass cross-section [4]

2.4.4 Chemically strengthened glass

Another process leading to an increase in a load bearing capacity of glass is the chemical strengthening. In this method, the prestress is introduced by dipping the glass sheet into an electrolysis bath in which sodium ions are exchanged for potassium ions. Potassium ions are 30% larger, forming a pressure strain on the outer layer. This type of glass can go through processes of cutting, drilling or edging even after the strengthening process. Another advantage is the absence of thermal deformation. However, a relatively thin layer of surface tension causes little scratch resistance, and also, compared to tempered glass, the production of chemically hardened glass is more expensive.

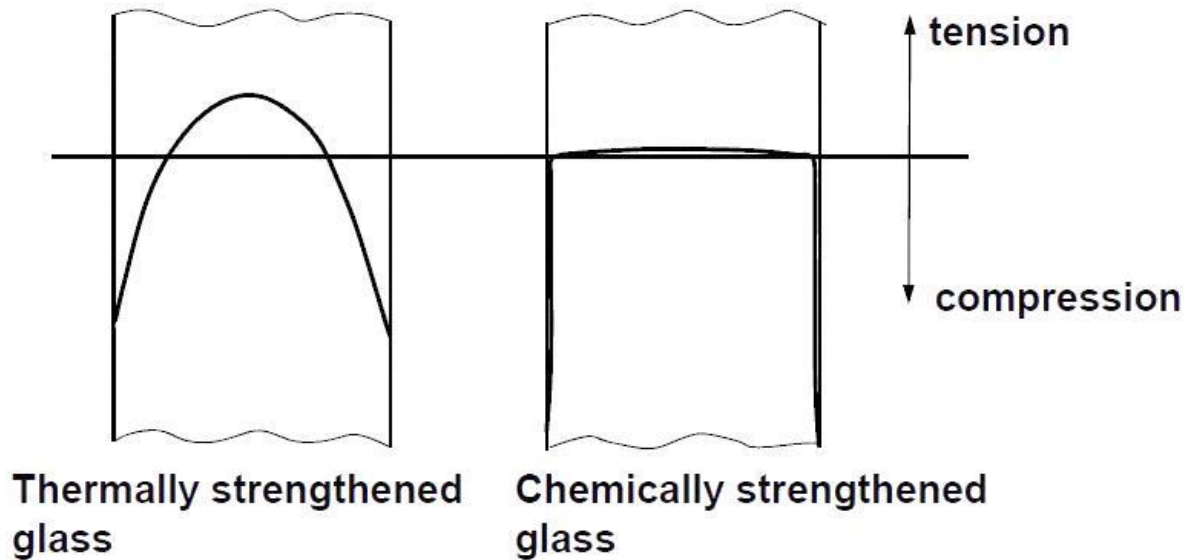


Figure 2.7: Comparison of stress distribution in cross-sections of tempered and chemically strengthened glass [2]

2.4.5 Laminated glass

Lamination is a process in which two or more glass panes are attached to each other. For laminated glass are used as float glass as well as heat-strengthened and tempered. The main advantage of this type of glass is the way of breaking. When it cracks, it remains stuck to the bonding layer, so it is possible to consider the residual capacity of the entire panel [9]. Laminated glass has a great use for glazings overhead, production of windshields and bulletproof glass.

As an interlayers in laminated glass the most common are materials as follows [2,11]:

- polyvinyl butyral (PVB)
- Thermoplastic polyurethane (TPU)
- ethylene vinylacetate (EVA)
- Polyester (PET)
- Cast in Place (CIP) liquid resin
- Ionoplast

The most common interlayer is PVB foil, with basic thickness of 0.38mm. More than one foil can be used as a bonding material. In the production of PVB-bonded laminated glass, the layers of glass and foil are set in a predetermined order, preheated to 70 ° C, and pressed between the rolls where the air from in between the layers is squeezed out. Subsequently, the laminated glass is transferred to the autoclave and heated to 140 ° C under a pressure of 800 kPa in a vacuum bag [2]. Because PVB is a viscoelastic material, its mechanical properties strongly depend on the temperature and the load-acting time. For this reason, the interaction between individual layers can not be taken into account for the long-term load.

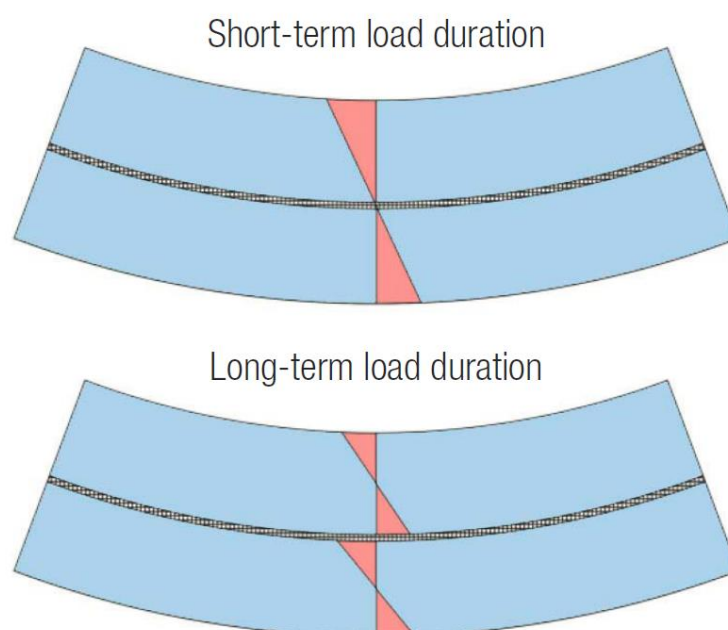


Figure 2.8: Behaviour of laminated glass according to duration of load [2]

Another method of lamination that is relatively wide spreaded in the construction industry is the use of cast in place liquid resins. During application, the glass panes are vertically stored with a constant predetermined gap (e.g., 2mm), which is then injected with liquid resin. Using this method of lamination, even large sized glass plies can be joined in a sufficient way. The advantage of using resins as interlayers is in achieving better acoustic insulation [9].

For glass used in areas where sudden burdens can occur, such as hurricane, the requirements for its strength and safety are more demanding. For these reasons, SentryGlas

Plus (SGP) ionoplast interlayers are used in the laminated glass. These films are applied in autoclave, similarly to PVB films [1]. SentryGlas Plus (SGP) is manufactured in 0.89 mm, 1.52 mm and 2.28 mm thick sheets or in 0.76 mm and 0.89 mm rolls. The advantage of SGP is the stiffness up to 100 times higher than PVB foil, which significantly reduces the deformation after glass breaks [1]. Also, higher permanent temperatures (up to 70 ° C) change the mechanical properties only minimally, and it is possible to consider the assembly as one element even for the long-term load [1]. On the other hand, it is necessary for the long-term actions take into account the stress evolved from the change of temperature, as the SGP thermal expansion is significantly higher than the one of glass.

Between the single plies of laminated glass elements like decorative, thermotropic, electrochromic or electrophoretic interlayers can be installed. Those affect the transmission of solar radiation and hence the thermal gains of the glazed building. With the development of renewable sources of energy, photovoltaic cells are being applied in interlayers.



Figure 2.9: Photovoltaic cells located in the interlayer of laminated glass [1]

2.5 Coating the panes

One of the methods frequently used for influencing solar gains and transmission of both visible and invisible parts of light is applying thin film coatings. Metallic coatings also effect colour appearance of glass where it was used. Those films are applied in processes as follows:

- on-line (hard coatings)
- off-line (soft coatings)

The mechanical properties remain generally unaffected by the coating process [1,2].

2.5.1 On-line coatings

This type of coating is applied to glass in annealing lehr while the glass is still fluid, which leads to longer durability of film. On the other hand hard coating films comes in smaller variety.

Pyrolytic hard coatings withstand also processes like bending, tempering and enamelling and significantly improve solar control properties of glass and therefore are used for thermal insulating glass and self-cleaning glass [1]. When a coat of metal oxide together with a layer of tin oxide is applied, it reduces the emissivity (heat radiation) of the glass pane from 90% to 15%. In reflected light then the panes may appear to have a colour-tinted metallic sheen [1]. For keeping its self-cleaning feature, glass pane with this type of film applied to its surface can't be contaminated with silicon sealant.

2.5.2 Off-line coatings

Soft coatings are applied to surfaces of glass in its solid state. It can be to both jumbo sheets or panes already cut to needed shape. The coating may be applied by dipping or by a vacuum deposition process [2]. Very often used method for off-line coatings is magnetron sputtering. Compared to on-line coatings tempering, drilling or cutting out has to be done before application of these thin films. Nowadays, up to 15 different coatings can be applied. When used with insulated glazing units (IGU) off-line coatings are less durable than on-line,

and may have to be applied to the cavity facing surfaces of the glass, known as Surfaces 2 and 3. They are then protected within the glazing cavity [2].

Another process of improving properties of glass by coatings is dip coating. They can be classed as soft or hard depending on the temperature of subsequent heat treatment [1]. Main advantage is in reducing the reflection to 1%.

Reflection colour	Visible light [%]			Total radiation [%]		
	τ_v	ρ_v	α_v	τ_e	ρ_e	α_e
Pyrolytic (online)						
blue-grey	54	19	27	38	16	46
bronze colours	18	17	65	29	14	57
green	26	32	42	19	17	64
Magnetron sputtering (offline)						
intense silver	08	42	50	06	37	57
silvery	32	13	55	26	14	60
grey	40	10	50	37	09	54
intense blue	08	30	62	08	25	67
blue	50	07	43	45	08	47
strong green	07	30	63	04	17	79
green	26	11	63	15	08	77

Table 2.2: Optical properties of various solar control coatings [1]

2.6 Cutting, drilling and grinding

Processes of cutting, drilling, edge and surface grinding are done with multi-point tools and usually take place before any other treatment of improving glass properties. For cutting the glass are used automatic diamond-tipped cutting arms and in modern plants glass up to thickness of 19 millimeters or laminated glass with thickness 2 x 8 millimeters can be cut [1]. For more complicated shapes and more thick glass panes the method of abrasive water jet cutting can be used. This is more accurate way of cutting, with accuracy of 0,3 millimeters depending on cutting speed and there are no restrictions in shape [1]. On the other hand, it is more time and money consuming.

Making of holes is done in the diamond drilling process by local grinding [1]. Drilling is done from both sides at the same time and maximum diameter of opening with normal tools

is around 70 millimeters. With special ones it might be up to 150 mm. Universally accepted rules for defining the distance between the hole and the edge and between the holes themselves are still not set [1]. Recommended ones are shown in the figure below.

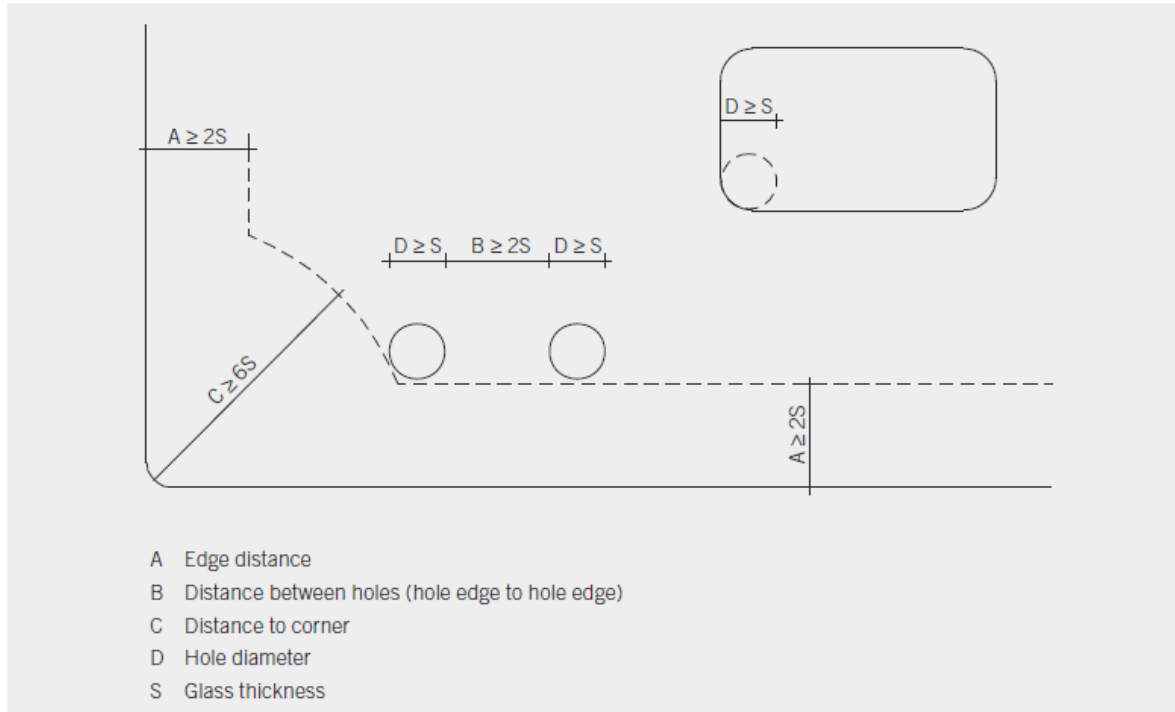


Figure 2.10: Recommended positioning of holes (conservative approach intended for guidance only) [1]

The processes of grinding and polishing are done by metal tools with a bonded coating of carborundum or diamond particles and happen in several stages with decreasing grain sizes until the desired optical and mechanical properties are achieved. The first stage is the seaming, arising and grinding of the cut edges. After fine grinding or smoothing, the edges of the glass have a flat, continuous matt appearance. The edges only become transparent after final polishing [1].

2.7 Glass structures connections

As the dimensions of glass panes are considerably limited, it is necessary to combine the individual components to create large dimensional elements, often designed in modern architecture in order to achieve a safe transfer of loads to foundations and then to soil. Whether it is the attachment of glass facades to a supporting part, usually a steel structure,

or the joining of individual segments of pillars or beams in large dimensional elements, it is necessary to carefully focus on detail design to avoid stress accumulation at these points leading to brittle fracture. For this reason, the requirements not only for the design, but also for the construction of the joints are high. To prevent creation of peak stresses plastic, resin, polyamide and light metal materials are placed in the contact area of glass and metals [9].

2.7.1 Glass load bearing structures

Linear elements

Those load bearing structures are axially stressed, both compressed and tensioned. In practice, the structures loaded as described are hinged columns or diagonals of paved trusses. The behavior of linear elements stressed by the combination of axial force and bending moment is still area for further research [9].

Glass panes

In general, the slabs are characterized by one dimension (thickness) significantly smaller compared to the other two dimensions and the loads usually acting perpendicular to their plane. Glass panes are used for flat glazing, or for staircases, balustrades, and various types of roofing. The design is affected by the shape of supports. For panes that are linearly supported on all edges and their deflection is larger than their thickness, the calculation must be based on the theory of large deflection in which the slab is considered as a membrane. The linear elasticity theory is uneconomical in this case. [9]

Beams

Beams are horizontal elements subjected to loading by bending moment around their strong axis. The bearing capacity of glass beams is limited by lateral torsional and local buckling and tensile bending stresses. They are used as simply supported or cantilevered. Maximum length of glass beams is around 6 meters [4]. Sometimes the glass is combined with other material to form a hybrid beam. Other materials such as timber, concrete or steel create flange while glass forms a web of a beam [9].

Glass fins

Vertical load bearing elements, oriented perpendicular to the glazing plane of building envelope, called glass fins, serve as reinforcements of glass facades and provide the transfer of load from the wind to other supporting elements of the structure. Glass fins are mainly loaded by bending moment. The fins of more than 8 m span are executed as top-hang, shorter ones are bottom supported. For joining the fin and the façade's pane, silicone-bonded joints or screw connections are used [9].

2.7.2 Types of connections used in buildings

The most widespread types of glass joints are bolted joints. However, architecture of nowadays is increasingly focusing on the minimal visual effect of connections, so research takes place in the development of adhesive joints that create the appearance of uninterrupted construction. Thereby the attractiveness and impressiveness of such structures is increased. The most common joints of glass constructions are described in more detail in this chapter.

Supports of glass slabs

Linearly supported slab around its perimeter is one of the simplest supports for glass panes. In this type of support, glass is fitted into a frame made of aluminum, steel, plastics or timber. The disadvantage of this solution is the uneven distribution of stresses along the support which must be taken into account in design [2]. Other types of panel support include local edge support, structural silicone seal and local point support [4].

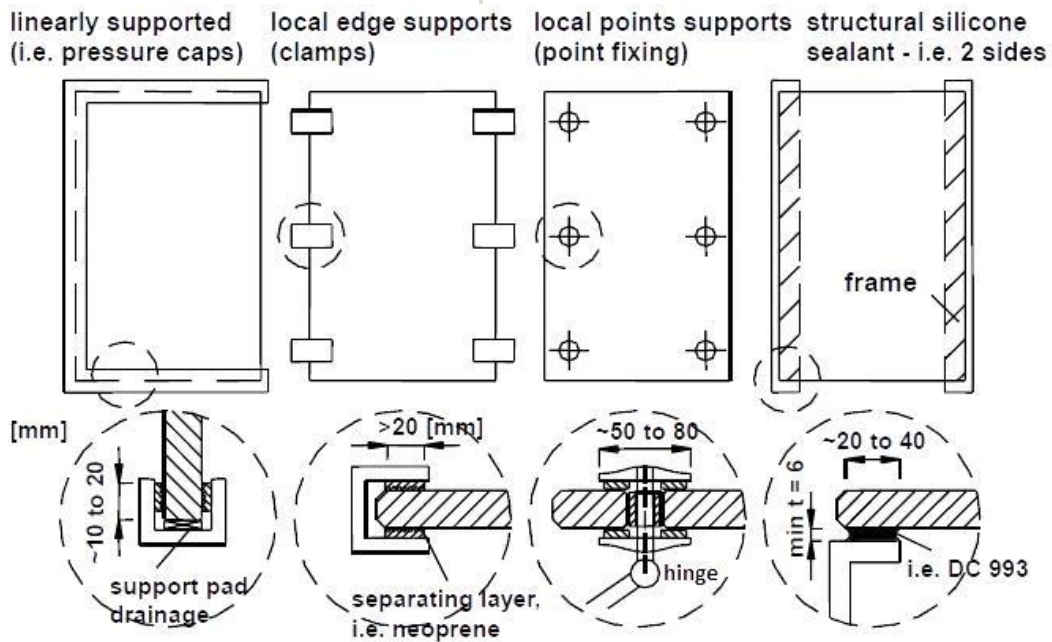


Figure 2.11: Types of supports of glass slabs [4]

Standard bolt connection – shear bolt

This is the simplest joint of the glass structures, where the bolt's head protrudes from the glazing plane. The load is transmitted from the glass to the screw through the inner flexible material. The contact surface is very small, therefore the load capacity is smaller, compared to other types of joints. Because the glass element is firmly attached to the support structure, this makes it almost impossible to move. Therefore, local peak stresses occur around the bolts [9].

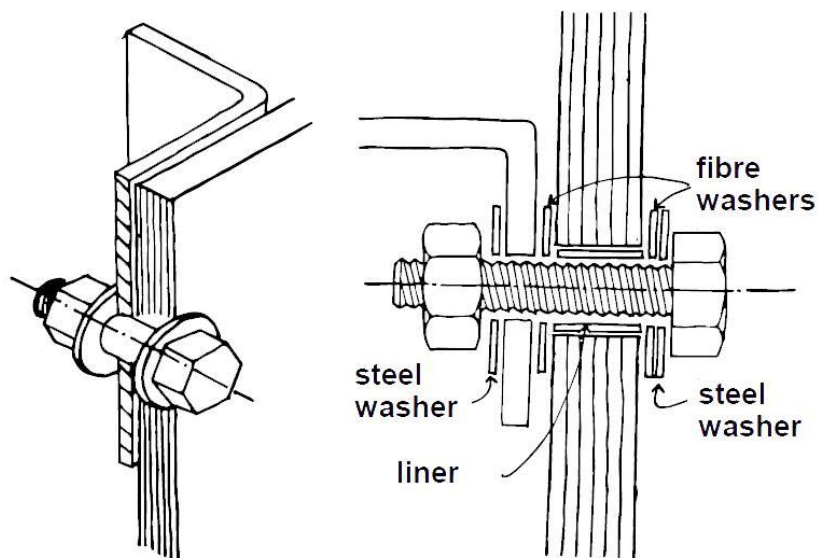


Figure 2.12: Standard bolt connection – shear bolt [4]

Simple countersunk-head bolt

This type of joint is similar to the previous one. The main difference is that the bolt's head is recessed in a plane with a glass plate. Also in this connection, local peak stresses are generated around the bolt. The described connection does not allow ratification between glass and steel.

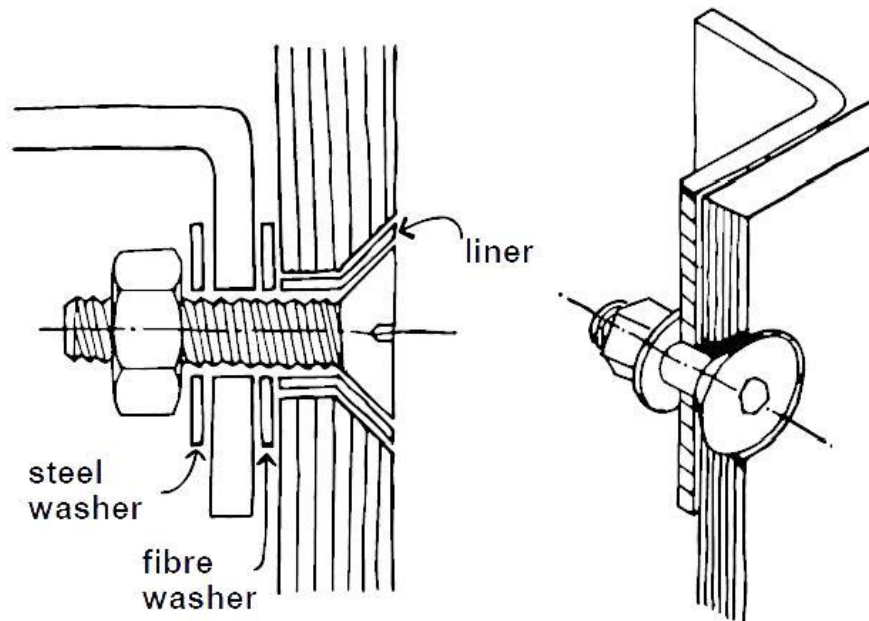


Figure 2.13: Simple countersunk-head bolt [4]

Bolted connection with steel splices

In this type of joint, steel splices are added on both sides of the glass pane, which are firmly connected by the bolts, so there is no mutual displacement between the glass and the steel plates. The opening for bolt may be larger than the diameter of the screw, which makes it possible to align the glass sheet when assembled. In practice, the joint is made using pre-tensioned screws tightened to the prescribed stress by a torque wrench. Load transfer occurs through friction between the steel and the glass, therefore the contact surfaces must be suitably adjusted and flexible material (plastics, neoprene, etc.) must be inserted between the glass and steel.

The latest research, however, point to the negative impact of the friction joints used in the laminated glass, where the interlayer is squeezed out at the joint site and consequently the mechanical properties of the laminated glass are changed [9].

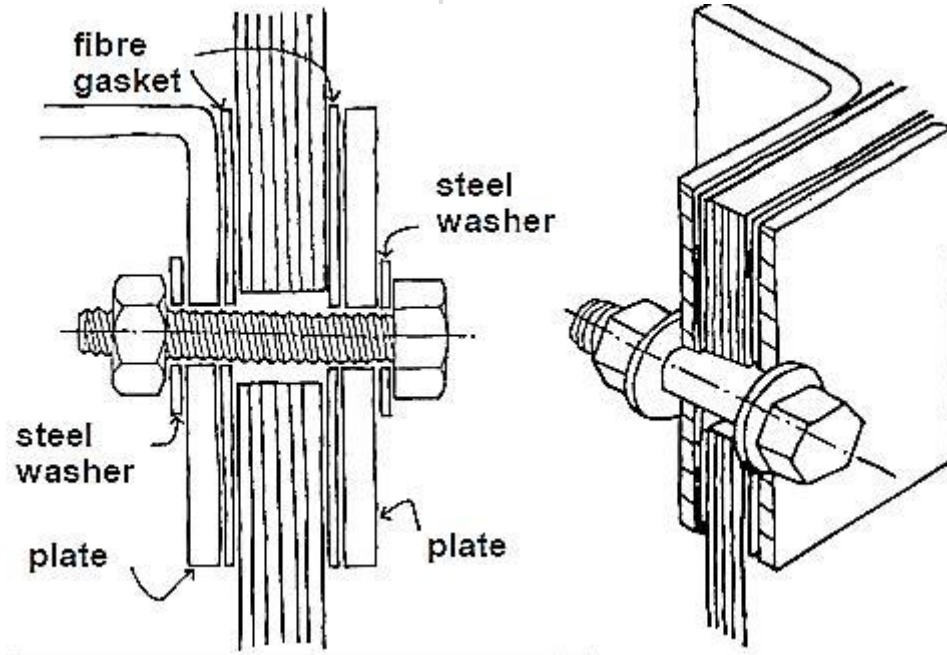


Figure 2.1: Bolted connection with steel splices [4]

Bearing bolts with steel splices are suitable only for tempered or heat-strengthened glass. In this type of connection load is transferred directly from glass pane through interlayer to bolt. Load bearing capacity depends on number of bolts and their diameter. The scheme and behaviour of such connection is illustrated in the figure below [4].

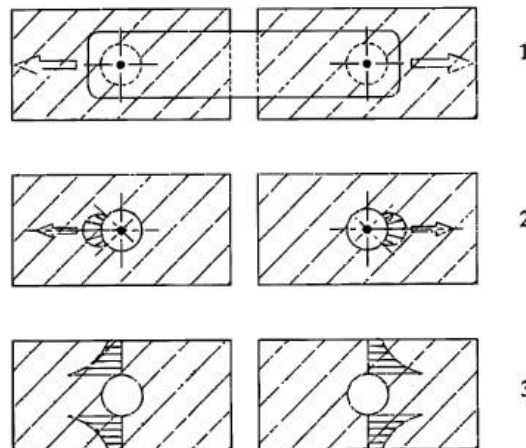


Figure 2.14: Bearing bolt connection with steel splices [4]

- 1) Scheme of the connection
- 2) Compressive stress in the glass pane
- 3) Tensile stress in the glass pane [5]

Bolted connection with stud assembly

The main advantage of this type of connection is the transfer of vertical load by a stud that is part of the connecting steel plate. This stud is larger in size than the bolt, which leads to higher pressed area and to lower stresses in glass. The horizontal load is transferred by countersunk-head bolts. The diameter of holes for bolts is larger than the bolt's diameter to prevent the in-plane load being transferred by them. The disadvantage of the joint is the need to drill more holes in the close proximity [9].

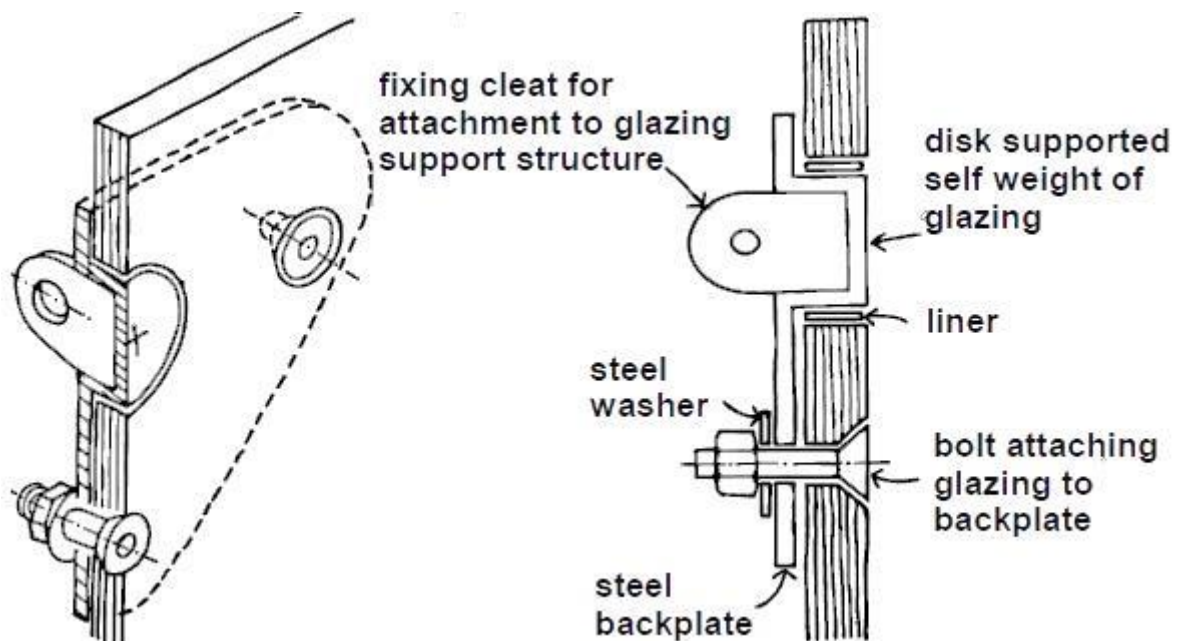


Figure 2.15: Bolted connection with stud assembly [4]

Spider connection

Spider joints are used for connecting the individual glass panes of facades to supporting structures. This joint may have one, two, three or four cantelivered arms that extend from the center. The steel part of connection is attached to supporting structures. The advantage of this type of joint is the possibility of partial rotation of the glass pane using flexible profiles not only in the opening itself but also brackets. This adjustment reduces the moment transmitted by the glass pane, resulting in a more economical design of the joint [9].

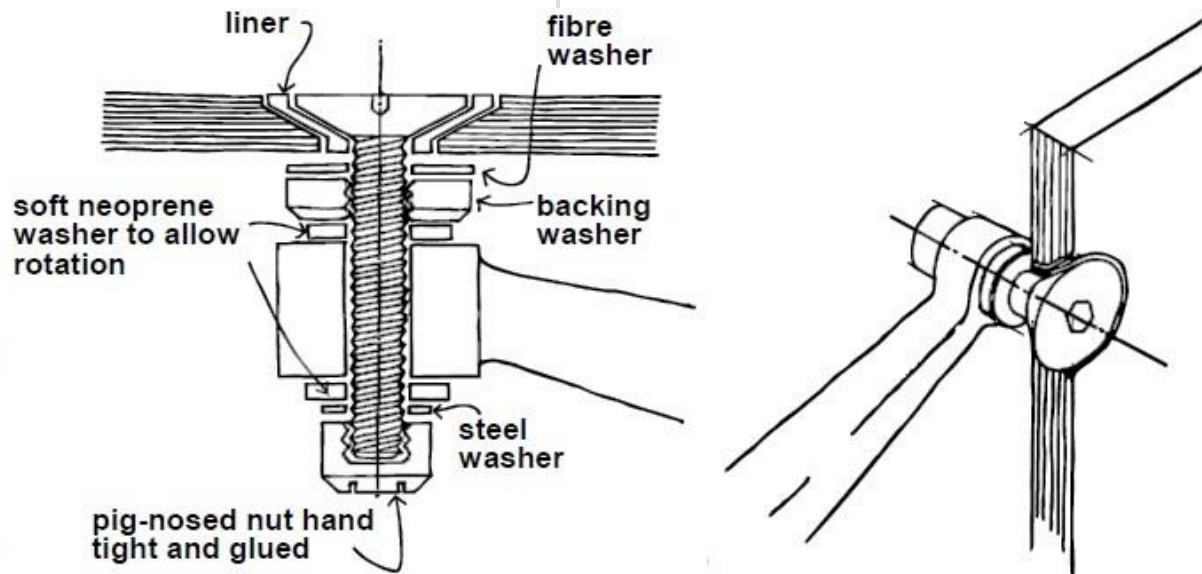


Figure 2.16: Spider connection [4]

Bonded connections

The bonded joints according to the type of adhesive used are divided into elastic (silicone) or hard (resin). The main advantage of bonded connections is the distribution of stresses in the vicinity of the joint where, unlike the bolted connections, the local stress peaks do not occur [2]. Further advantages such as weight reduction, the ability to connect thinner materials, the possibility of bonding and, at the same time, sealing and aesthetic enhancement contribute to the development of these less researched areas of glass connections [4]. The design should take into account the minimum shear stiffness of the flexible adhesives, as well as the influence of the temperature and the length of the load to its strength. Also, decrease in stiffness shall be noticed due to aging of the adhesive.

It should be also said that the behavior of adhesive bond strongly depends on a type of adhesive and the thickness of the adhesive layer. The following are the mostly used adhesives [5]:

- Cyanoacrylates
- Modified epoxies
- Polyurethane resin
- Structural silicones

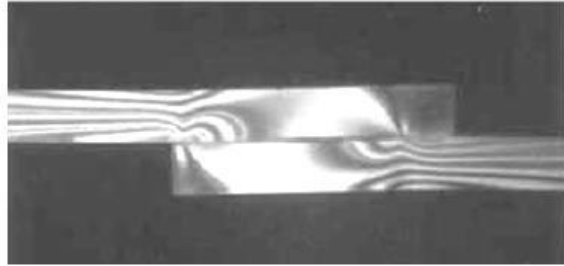


Figure 2.17: Stress distribution in connection made with hard adhesive [4]

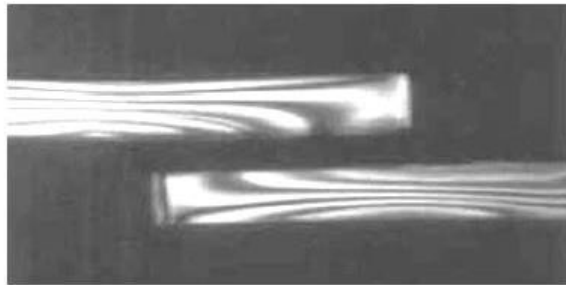


Figure 2.18: Stress distribution in connection made with thick elastic adhesive [4]

3 The aim of master's thesis

As mentioned in the previous chapters, very common form of connecting the glass components to each other or to different primary load bearing structures made of materials like steel, concrete or timber is bolted connection, for which is necessary to drill holes into glass plies. Those openings negatively influence the load bearing capacity of glass component. Nowadays very popular all-glass structures where the glazing (secondary load bearing structure) is joined to the glass beams with holes as primary load bearing structure, are designed in dozens all over the world, but there is not generally accepted guide for determining the hole to edge distance according to the way of loading.

The essential to this master's thesis is to provide the designers with the information of a stress distribution around openings and describe the way of how it changes according to variable diameter of the hole and different distance of the edge of the hole to the edge of the ply.

To determine the behavior of glass beam with two vertically placed openings and the stress distribution in close proximity of the holes, two methods will be used:

- Experimental analysis
- Numerical analysis

Also a parametric study will be performed to find out how different input parameters like diameter of the holes and hole to edge distance affect the stresses in the researched area.

4 Experimental analysis

The experiments were held indoor with room climate conditions. Temperature was around 19°C. For the experimental analysis 3 specimens made out of heat-strengthened glass were used, numbered N01, N02 and N03. Climate conditions during the test of each specimen were similar and thus, the results are not influenced by different temperature or humidity. The tests were running until the failure of a structure. The specimen numbered N04 made out of annealed glass is a part of the project named “The effect of openings on stress distribution in glass beams” but is not covered in this master’s thesis. This specimen will be tested by the method of photoelasticimetry later this year.

4.1 Testing equipment

4.1.1 MTS QTest 100

The floor model testing frame with TestWorks 4 software was used to apply the load to the glass beam. This model of test frame is equipped with the crosshead and has loading capacity up to 100 kN.



Figure 4.1: MTS QTests 100

4.1.2 Rod-type borehole extensometer

Four rod-type borehole extensometers were used to measure vertical deflection. Two of them were placed on the steel carobs in the middle of span of beam and the other two recorded vertical deflection at the point above the supports. They were placed directly on the edge of glass.



Figure 4.2: Rod-type borehole extensometer with magnetic holder

4.1.3 Dewetron DEWE-5000

For recording measured values benchtop measurement system Dewetron DEWE-5000 with 16 DAQP isolated analog input amplifier modules and with DEWEsoft software was used [18]. During the measurements values from 8 strain gauges, 4 rod extensometers and force were recorded.



Figure 4.3: Dewetron DEWE-5000 with DEWEsoft software [18]

4.1.4 The "2 x IPE table"

The table is composed of 2 IPEs joint together through top deck made out of 10 mm thick steel plate. Width of the table is 400 mm. Bigger dimensions of the table widen the stable area for testing which increase the total possible size of tested specimens. Described structure can be seen in the figure below.

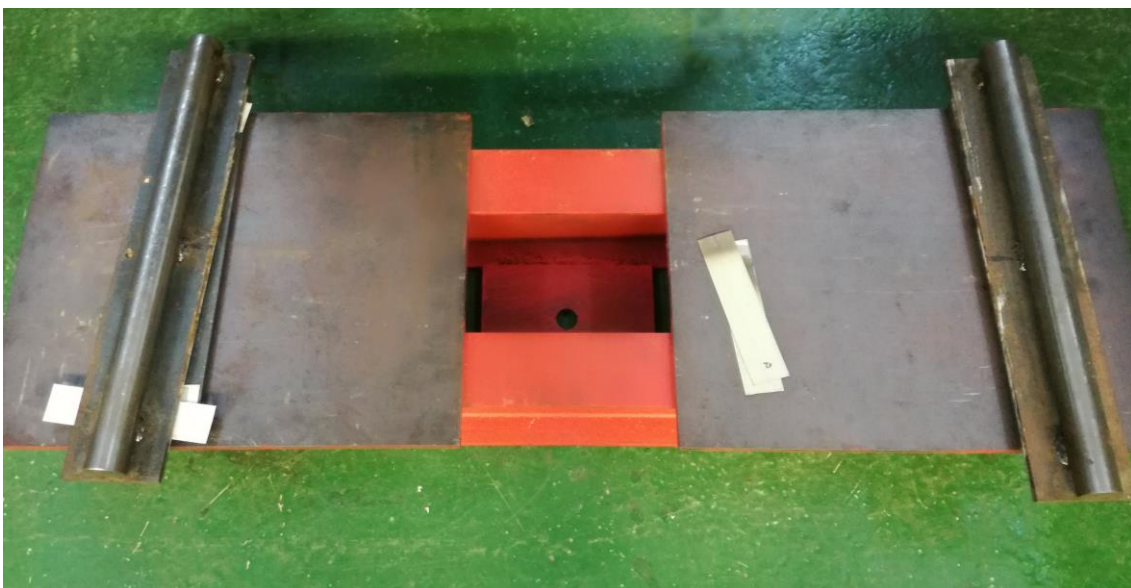


Figure 4.4: The table with cylindrical supports

4.1.5 Lateral buckling restraint

Two identical steel structures were designed and fabricated in order to restrain a specimen from lateral buckling. The lateral buckling restraint is composed of 3 parts. The lower steel plate is designed to be joint to the “2 x IPE table”. Two pairs of bolts on each side keep the plate in place. The position of 2 upper parts to the lower part can be changed, which allows using the lateral buckling restraint for testing specimens of different thicknesses. The construction is showed in the figure below.

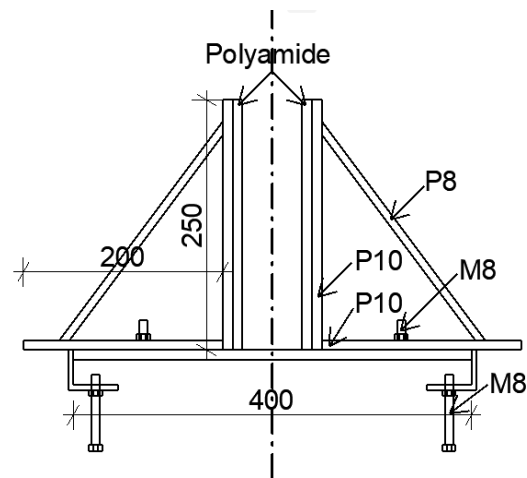
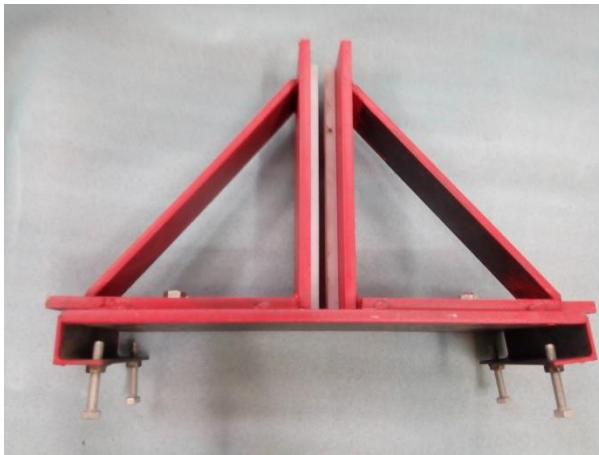


Figure 4.5: Lateral buckling restraint (distance in mm)

4.1.6 The loading cell

The loading cell is composed of steel section UPE 160 and two steel tubes TR 48,3/4, which are vertically reinforced by steel plate in the points where peak stresses were expected. The distance of tube's centers is 300 mm. During the tests, the construction was design to be connected to crosshead by 4 threaded rods M8 and two steel plates noticeable in the *Figure 4.10*. For the design of the loading cell parts their total load bearing capacity was taken into account as it has to cover whole force range which can be generated by the floor model testing frame MTS QTest 100.

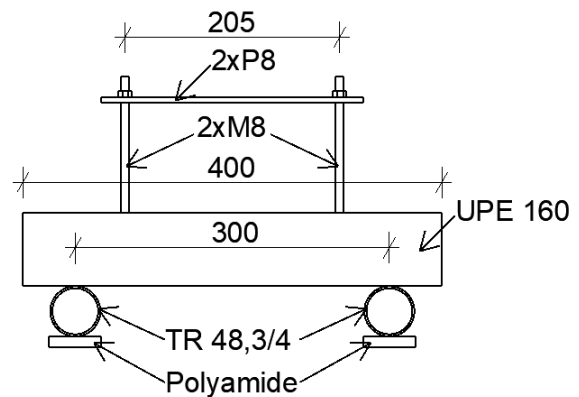


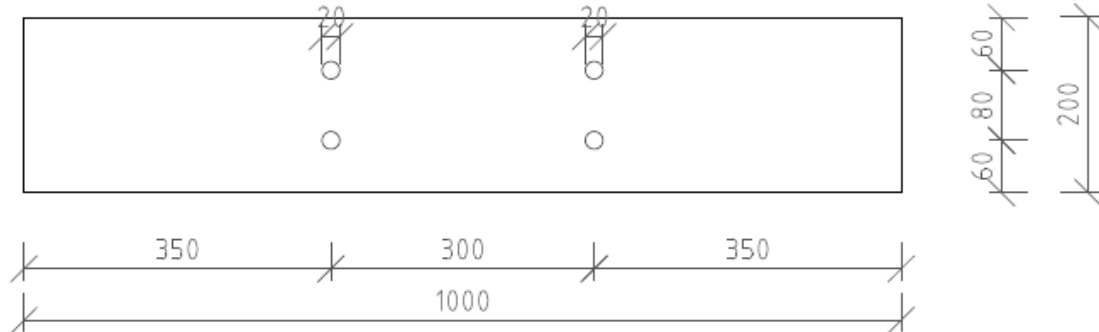
Figure 4.6: The loading cell (distance in mm)

4.2 Geometry of the specimens

All three specimens were made out of heat-strengthened glass of thickness 12 mm with suggested minimal characteristic strength of glass 70 MPa. The beams were asked and fabricated in dimension 1000 x 200 mm. In the distance of 350 mm prepedicular to shorter edge two holes of diameter 20 mm were drilled above each other. From the longer edge the holes are 50 mm far and the distance between the centers of the openings is 80 mm. The specimens are symmetric, which means, that there are 4 openings in total. The center to center distance of supports is 900 mm. Cylindrical supports are placed 50 mm from the edge of the beam from both sides. The tested beams represent the cut of real structures. Beams of similar geometry as the tested once can be found in structures of roof glazings or pedestrian bridges. In real constructions of this shape, a beam, is primary load bearing structure, supporting an impermeable glass roof or a top deck of a bridge. Drilled holes are ready for insertion of bolts, by which secondary load bearing structure is connected to a beam. In reality a load is introduced to the beam through joint, in this case, bolted connection, thus the forces

will act on a beam in the same position as in this analysis.

1:5



TEPELNĚ ZPEVNĚNÉ SKLO tl. 12 mm, 3 ks
PLAVENÉ SKLO tl. 12 mm, 1 ks

Figure 4.7: Drawing from the providing documentation of the glass beams

As described in the previous chapters, I designed the special steel constructions which later were made for the experiment to prevent the glass beam from lateral buckling and torsion, as it was loaded in vertical position. Assembly of the steel structures with the specimen placed in it is obvious from the following figures.

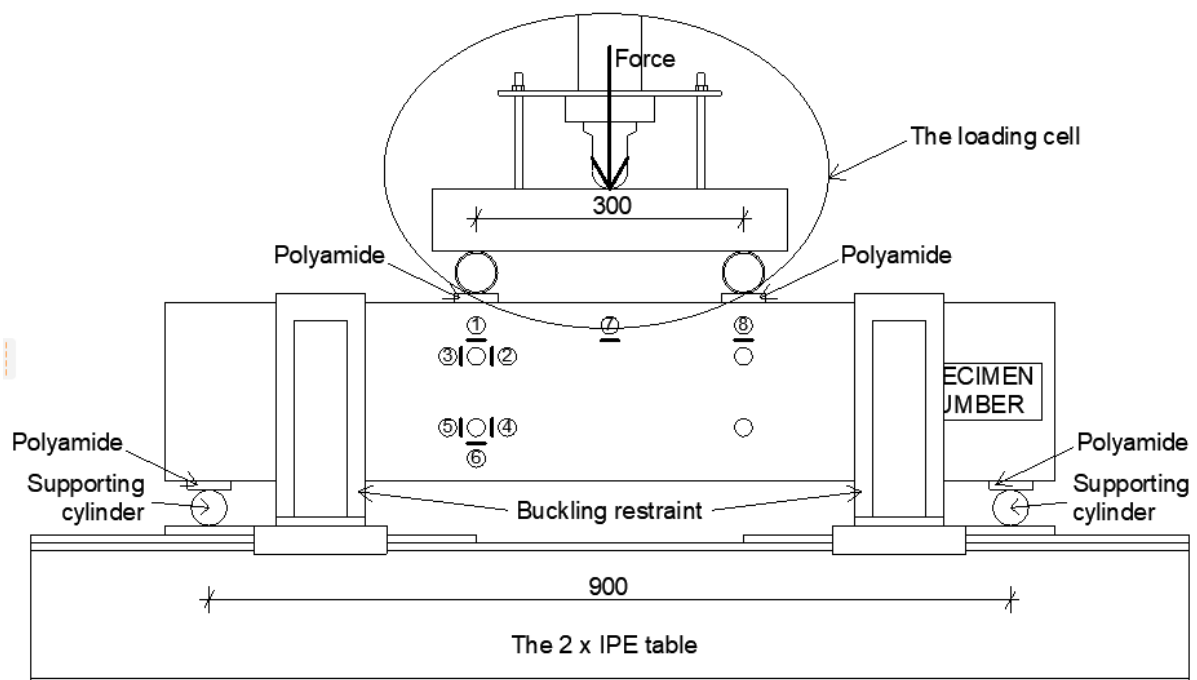


Figure 4.8: Scheme of the loading assembly (distances in mm)

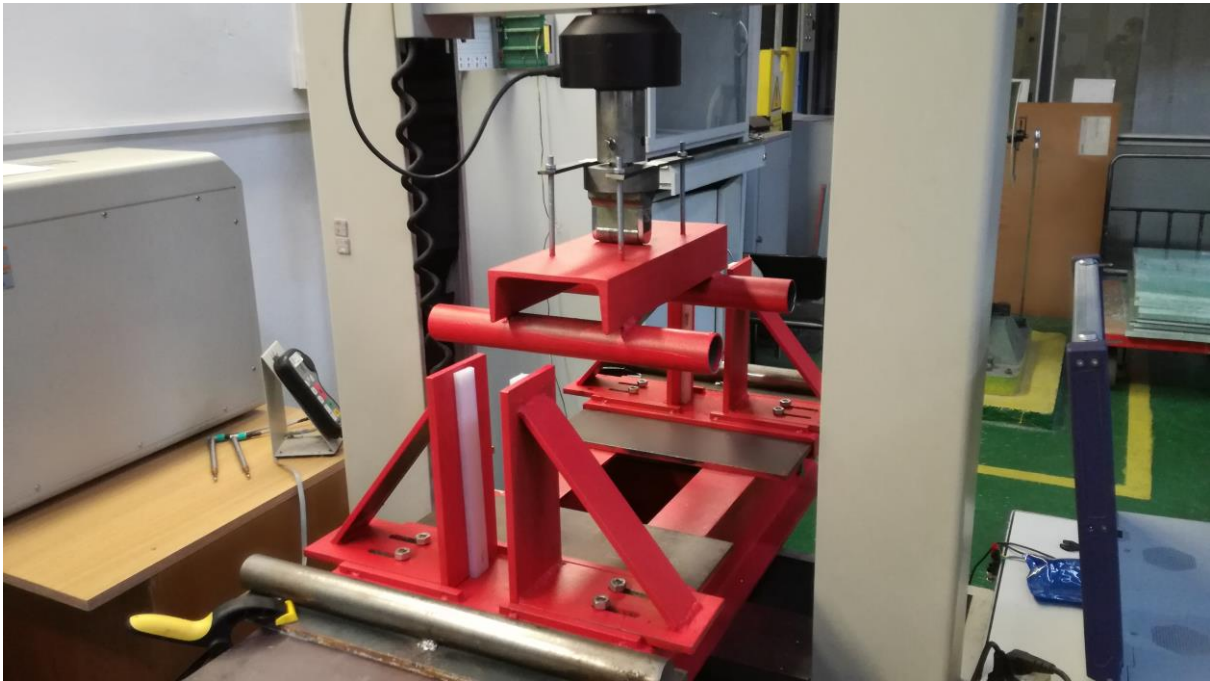


Figure 4.9: The loading assembly ready for specimen insertion

4.3 Testing procedure

All the equipment mentioned in the previous chapter was used for the tests. Loading force was generated by MTS QTest 100 machine. The role of steel parts was to keep the specimens in place and restrain the beams from other than vertical deflection. The experiments were provided on specimens which acted like simply supported beams. Glass beams were tested in four point flexural test. Force was introduced to the beam through steel cylinders specially designed for those experiments. Use of hollow cylinders with vertical reinforcement in the place of concentrated load allowed the force to act in the certain point. For providing hinged support, two solid cylinders were used. To prevent from creation of peak stress, in contact areas between the steel structures and glass, polyamide stripes of 10 mm thickness were introduced.

4.3.1 Four point flexural test

Four point flexural test leads to constant moment in between the forces. The consequences of moment distribution as described is that the crack will appear in the

weakest point of the specimen. Then, from the crack pattern of a broken specimen is obvious in which point stress exceeded the load bearing capacity of the specimen the first.

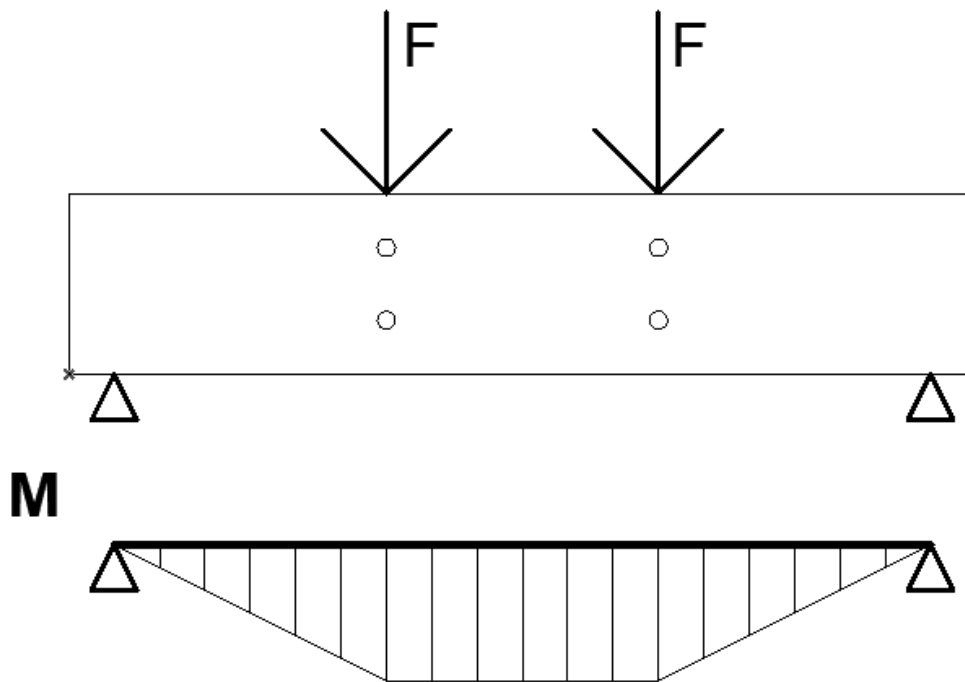


Figure 4.10: Moment distribution in four point flexural test

4.3.2 Strain gauges placement

For the evaluation of the stresses, resistance tensometry was used. Strain gauges were placed on the surface of each specimen. Geometry of the specimens was studied carefully and areas where strain gauges were glued was chosen in addition to the limited slots in Dewetron DEWE-5000 machine for recording the electrical resistance of each strain gauge, which later can be recalculated into strains and then into stress.



Figure 4.11: Measured values during the tests

During the tests held in January the Dewetron computer with 8 slots available for strain gauges was used. The symmetry of the tested beams was used and stresses were measured around the holes on one side with six strain gauges while on the other side there was one strain gauge placed to control the symmetry of loading. The most important areas of the research are around the openings thus, the biggest amount of the strain gauges is placed around them. The area where strain gauge was glued has to be at first cleaned and all oils and greases have to be removed from the surface of glass. For attaching it to the surface of the glass, the special glue was used. Then thin foil is placed over the strain gauge and by the pressure of hand air bubbles are squized out from below the strain gauge. The glue dries in the contact with air. All used strain gauges measure the deflection only in one direction.

Strain gauges were glued identically to each specimen. The figure below shows the directions of strain gauges with marked distances from each strain gauge to the closest edge of the beam.

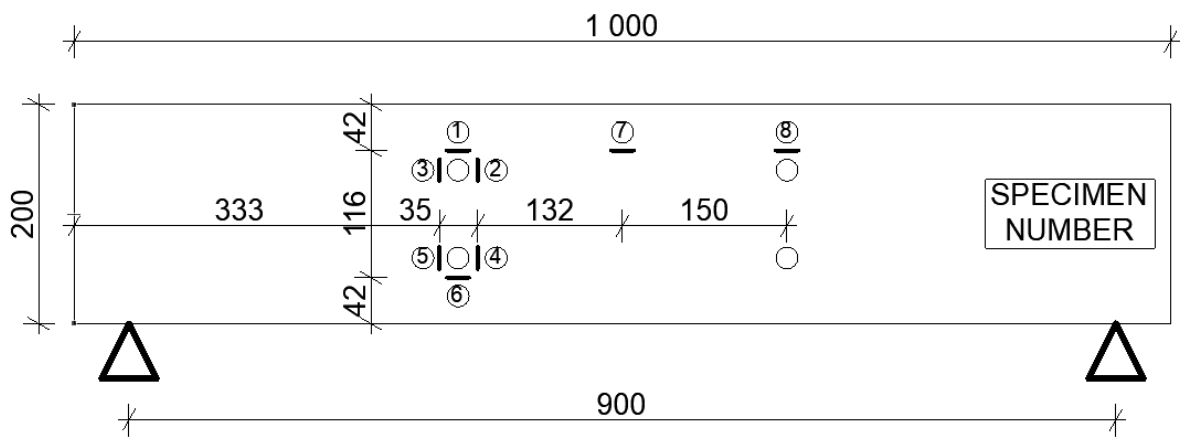


Figure 4.12: Location and orientation of strain gauges (distances in mm)

① – Number of strain gauge

4.3.3 Measurement of vertical deflection

Vertical deflection was measured by 4 rod extensometers. Two of them were placed in the middle of span from each side of the beam. Rod extensometers were placed on the horizontal plate of the two L-shaped steel components. Measuring the deflection from both sides allowed us to observe, if the beam buckles.



Figure 4.13: 2 rod extensometers placed on a L-shaped steel component

Other 2 rod extensometers were placed on the top edge of the specimen at the point above the supports. As there were plastic washers from polyamide inserted between the steel supporting cylinder and the glass beam, the deformation of the polyamide showed as significant. To obtain the real deflection of the beam in the middle of its span, vertical deformation measured in the center must be subtracted by the vertical deformation measured by extensometers placed at the points above the supports. From the figures below is obvious how glass beam is pressing into the polyamide pad by the lift of the edges of the plastic washer.



Figure 4.14: Rod extensometer above the support and noticeable pressing of the beam to polyamide

4.3.4 Failure expectations

The failure of glass structures is brittle and occurs immediately after a maximum load bearing capacity of an element is reached. Shards of heat-strengthened glass are similar to those of float glass, which allows us to fold the broken pieces of each specimen and determine where the crack was initiated, furthermore where the maximum stress was developed during the test. As for the experiments were used one ply beams without any further foils or additional layers added to its surfaces, collapse of whole structure and no residual strength are expected. According to the knowledge of the behaviour of glass structures know yet, the initiation of a crack is expected to appear in the area in close proximity to the points where the forces are introduced to the beam due to tensile stresses exceeding the load bearing capacity of the beam caused by compressive force. Also it could appear around the discontinuities in geometry, the edges of holes, due to tensile stresses overstepping its strength in this areas.

4.4 Loading of the specimens

All four specimens were required in the exactly same dimensions without any errors in manufacturing process. Initial measurement of each specimen indicated that OGB company provided very accurately made glass beams.

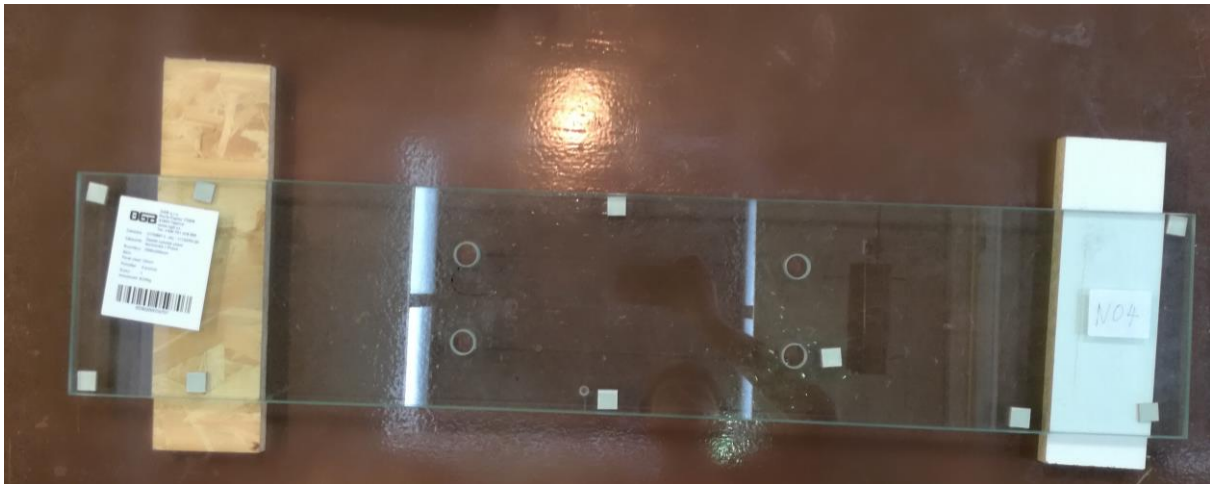


Figure 4.15: Specimen N04 before testing

Expected maximum load and vertical deflection were approximately estimated before the test. Also deformation of plastic washer was taken into consideration. During the experiment the deformation of polyamid showed as significant, thus during loading of the specimen N01, the right speed and a way of loading had to be found out by the method of few attempts. The floor model testing frame MTS QTest 100 loading allows to add and control the load by constant increase in vertical displacement.

N01

Total dimension and dimension of the openings of this specimen referred to required ones and no defects on the surface or edges were observed. For this beam four loading and unloading cycles were applied as during the first three attempts ultimate limit state wasn't reached due to significant deformation of polyamide. To avoid enormous pressing of plastic washer thin steel plates were added between the polyamide plates and supporting cylinders as well as in between the loading cell's tubes and polyamide plates attached to them.

During the fourth attempt the frequency of recording the measured values was set to 10Hz. The constant displacement of the crosshead of MTS loading frame was set to 0,4 mm/min. After reaching total vertical change in position of crosshead 1,5 mm, there was pause for 30 seconds. The pause was followed by the movement of the crosshead upwards to vertical displacement of 0,5 mm. After second 30 seconds pause, the specimen was pressed until reaching its ultimate limit state. Strain gauge number 3 was not recording the stress due to its defect.

N02

The specimen was perfectly manufactured regarding its dimension. No damages to its surfaces or edges were noticed, which may lead to weakening of the beam.

As the process of loading the beams was verified on the previous specimen and showed up as very efficient, the same loading speed was applied to the specimen N02. The difference to specimen N01 was, that at first, the displacement of the crosshead was 2,5 mm followed by 30 seconds pause and then total displacement was returned to 0,5 mm. After next 30 seconds pause, the specimen was pressed until reaching its ultimate limit state.

N03

The perfect condition of the specimen signaled, that the results won't be influenced by unprofessional manufacturing, transfer or storage.

The increase in total vertical displacement was set to 0,4 mm/min as in the previous specimens. After reaching the displacement of the crosshead of MTS QTest 100 gadget of 2,5 mm it was set to stop its movement for 30 seconds. Pause was followed by unloading and the arm reached displacement 1 mm. The following process was the same as in the previous specimens.

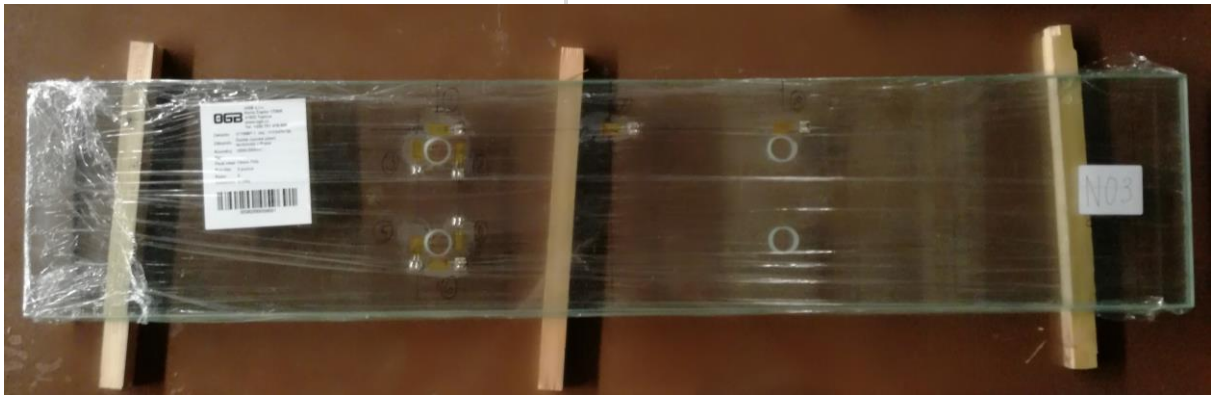


Figure 4.16: Storage of specimen N03 with glued strain gauges

4.5 Results

N01

The first specimen underwent 4 loading and unloading cycles, until its load bearing capacity was exceeded. Before applying the load, specimen was centered and its horizontal position was checked in order to load it symmetrically.

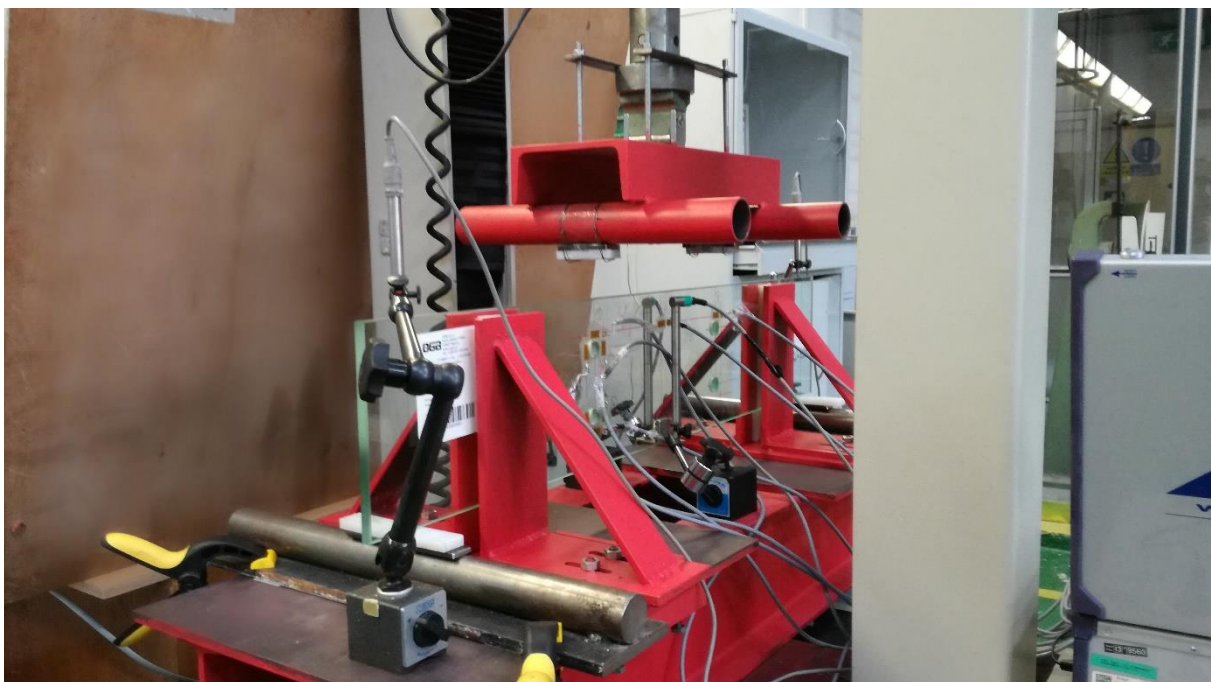
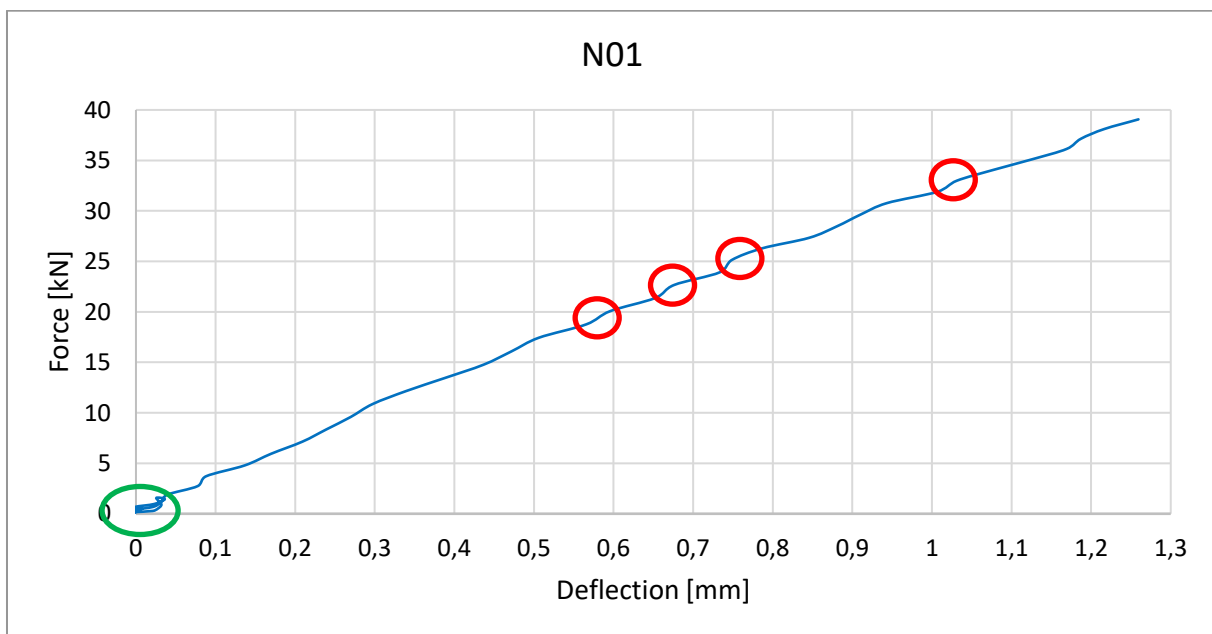


Figure 4.17: Specimen N01 ready for loading

In the process of test few non-linear deformations occurred. Those non-linear deformations marked red and seen in the *Graph 4.1* were presumably caused by polyamide

pads. After initial crack occurred, the collapse was brittle, which means the structure collapsed immediately without any warning. The maximum force reached was 39,06 kN. The process of loading to deflection of crosshead of MTS QTest 100 gadget 1,5 mm followed by unloading to 0,5 mm and subsequent loading is non-linear, due to pressing of plastic washers and delimitation of free space between the components. The clear vertical deflection of the glass beam, after subtracting the deformation of plastic washer reached 1,259 mm. The initial loading to deflection of crosshead of 1,5 mm followed by unloading part of the test is marked green, but the real vertical deflection of glass beam after subtracting the deformation of polyamide was only few hundredths of millimeters.

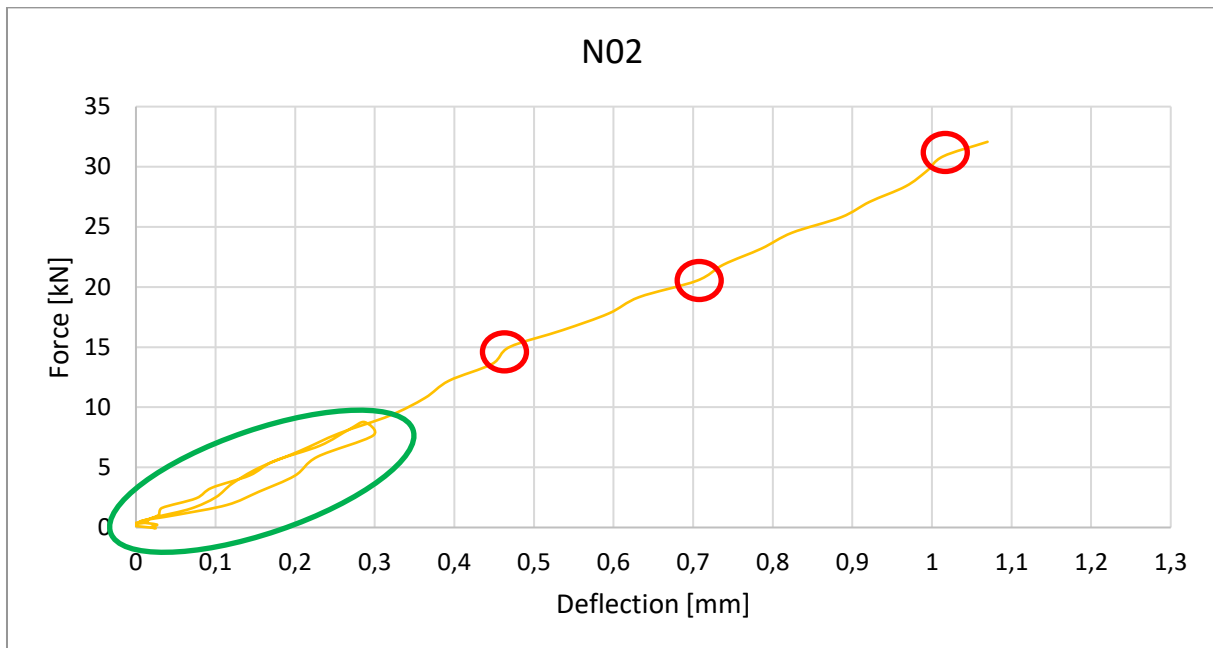


Graph 4.1: Force - deflection diagram, specimen N01

N02

The loading process of the specimen N02 was similar to previous one. The difference was in the initial cycle of loading and unloading, specifically speaking in the vertical deflections reached by the crosshead compared to specimen N01. Again, zone with initial cycle of loading and unloading is marked green and areas with non-linear behaviour are marked red in the graph. Also it is noticeable from the graph, that glass is elastic material, as after initial loading and unloading there is no initial deformation left. The maximum force reached is lower, compared to one needed for exceeding the load bearing capacity of specimen N01. The brittle collapse occurred at force 32,07 kN with the deflection of the beam 1,081 mm. Deformation

of polyamide washers is subtracted from the deflection measured in the centre of the beam, so the diagram shows the real vertical deflection of the specimen.



Graph 4.2: Force - deflection diagram, specimen N02

As reckoned, and known from previous researches, the heat-strengthened glass beam shards are similar to those of basic annealed glass. Thanks to dimensions of shards, it was possible put together each part of the broken glass like a puzzle and find out the point of initial crack. As showed in the figure below, the crack spreaded almost through whole ply and reached the edges.



Figure 4.18: The crack pattern of the tested beam

The crack began to spread from the point where load bearing capacity of the specimen was exceeded the first. In glass in general, such a point can be recognised by increased concentration of microscopic cracks. During the test the maximum stress occurred at the edge of lower hole and it is marked red in the picture below.

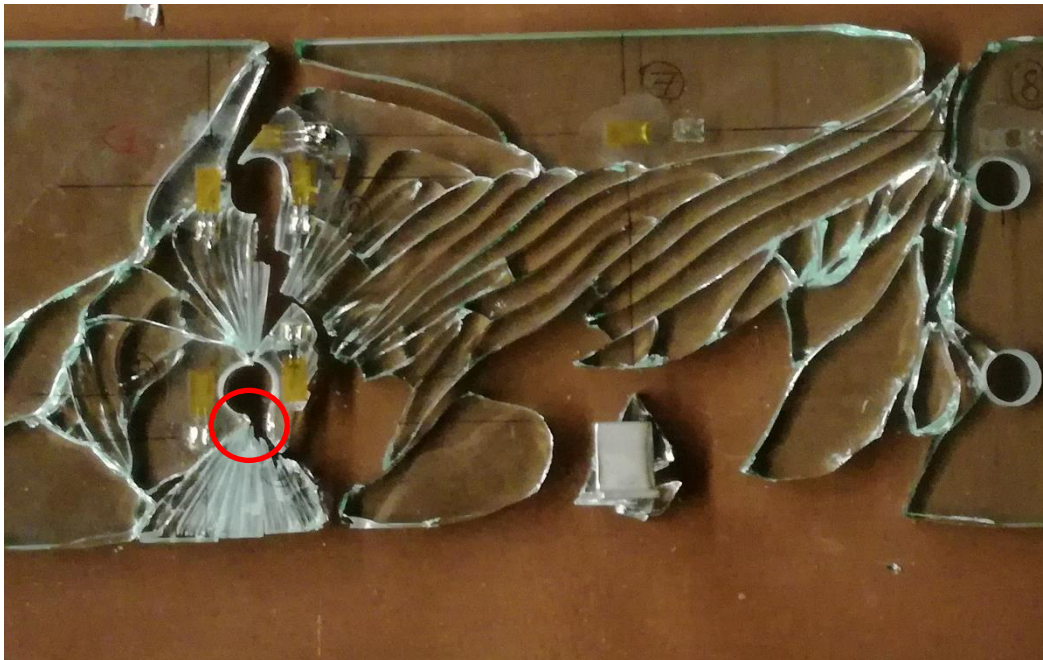
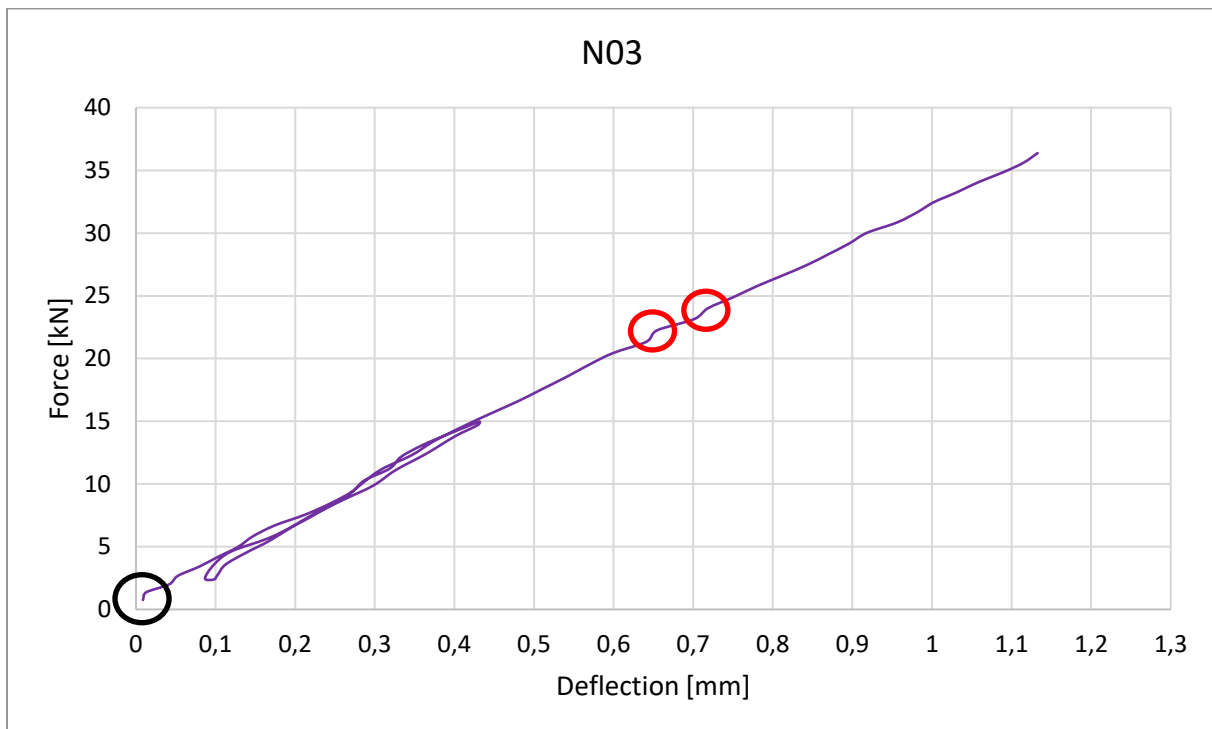


Figure 4.19: Point of the initial crack (marked red)

N03

The process of applying the load was similar to testing of specimen N02 and is described in previous chapters. Before starting the test and letting the MTS QTest 100 machine to load the specimen constantly by an increase in vertical displacement, the crosshead was approximated to the ply manually. To delimitate a free space between the polyamide plates and the glass beam small force lower than 1 kN was applied. Thus this minimal load can be seen in *Graph 4.3* as an offset of the line of diagram from the beginning, the point zero. By this approach non-linear increase in force and deflection in an inception of the test, which can be seen in the previous two diagrams for specimens N01 and N02, was eliminated. The offset is marked by black circle. The maximum force generated by the loading apparatus before brittle collapse of the structure was 36,38 kN. As in the previous graphs, the non-linear behaviour is marked by red circles. Specific for this specimen is, that some deformation remained after unloading to deflection of 0,5 mm in crosshead, which is not a

common behaviour of elastic materials such as glass. This recorded plastic deformation noticeable from the graph was presumably caused by the composition of steel supporting components, where delimitation of free space might happened and magnitude of mentioned deformation could be strengthened by the use of plastic washers. The maximum vertical deflection reached before breaking was 1,146 mm. The deflection shown in the diagram below is clear deflection of the glass beam as the deformation of polyamide washers was subtracted.



Graph 4.3: Force - deflection diagram, specimen N03

As in the specimen N02 the initial crack appeared at the bottom edge of the low left opening. The breakage was more powerful as it happened while bigger force was acting on the ply. For the crack pattern analysis it was not possible to put shards together, but the point of the crack initiation was obvious from both, the shards and the deflection recorded by strain gauges.

4.6 Comparison of specimens and conclusion

The *Graph 4.4* shows the difference in measured values between each specimen. Ultimate limit state was reached for each beam at different force and deflection aligned to

that load. Variety in maximum load applied to each specimen is presumably caused by the process of how heat-strengthened glass is produced (*Chapter 2.4*). As described in *Chapter 2.4.2*, due to fast cooling the surfaces are prestressed, which leads to higher strength of glass. During cooling temperatures may vary in few °C, thus the thickness of prestressed layer may be different to each heat cured glass pane which causes a variety in its strength. Comparison of values obtained from the tests and average value of force and deflection reached at breakage is shown in the table below.

	Max. force	Max. deflection	Stiffness
	[kN]	[mm]	[kN/mm]
N01	39,06	1,259	31,419
N02	32,07	1,081	29,914
N03	36,38	1,146	31,869
Avarage	35,84	1,162	31,067

Table 4.1: Maximum force deflection reached for each specimen

From the diagrams obtained from the measured data of each tested specimen, the structural and material characteristics of glass beams can be deduced. One of them is stiffness, which measures the resistance of elastic component to deflection, estimated from angular coefficients of linear trendlines created in Excel for force – deflection diagrams of each specimen. In the equations the stiffness of certain specimen is represented by linear coefficients standing by the unknown x . Estimated angular coefficients are as follows:

$$\mathbf{N01:} \quad y = 31,419x + 0,596 \quad (4.1)$$

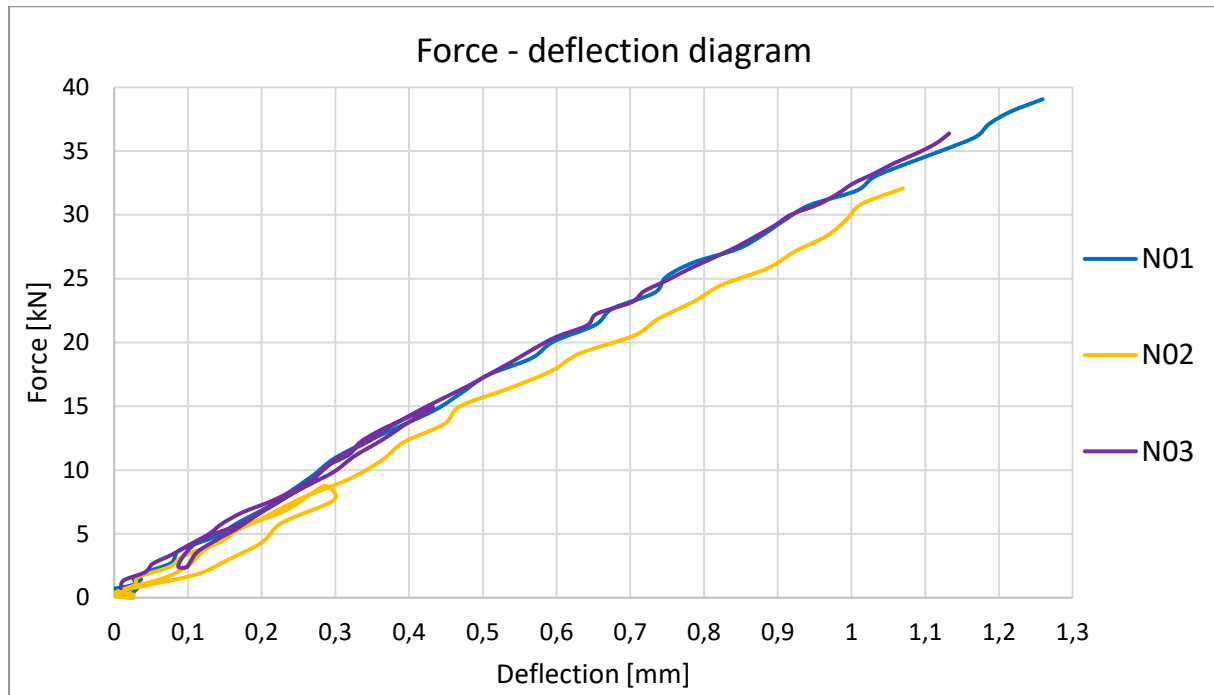
$$\mathbf{N02:} \quad y = 29,914x - 0,136 \quad (4.2)$$

$$\mathbf{N03:} \quad y = 31,869x + 0,757 \quad (4.3)$$

As shown in the diagram of comparison of force-deflection lines of all 3 specimens, the inclination of line of specimen N02 is different. The angle between the line and horizontal axis is lower which indicates lower stiffness. As all 3 tested beams have the same cross-section and length, Young's modulus is lower too, compared to specimens N01 and N03 which stiffnesses

are similar. This phenomena is presumably caused by different content of raw materials during its manufacturing process as modulus of elasticity is material property.

As all 3 specimens itemized slightly different values, for further calculations and modelling, average values will be used.



Graph 4.4: Comparison of all 3 specimens

As observed from the crack pattern of specimens N02 and N03, the initiation of crack was found at the edge of low left opening which signals that during the tests maximum stresses occurred at the described point.

As discontinuities influence the stress distribution in a significant way, it is vital for the future designers of glass structures to pay attention to those details. Moreover in real constructions, the bolts will be inserted in such holes, which may lead to even higher stress values induced by load acting on a structure at the area of close proximity of the opening.

5 Numerical analysis

For numerical modelling was used ANSYS Workbench 19.0 (student license) software. Mentioned software as one of many uses finite elements method (FEM) for analysing the structures. The Workbench interface provide easy orientation alongside conserving the high standard of ANSYS software [12].

The asset of creating numerical model is in money and time savings as number of specimens used is significantly reduced, while the results remain unchanged in quality. For beneficial numerical analysis is essential to collect data about real structures, to deduce mechanical properties of materials used in such components. After obtaining the characteristic of real structure from experiments provided, another step of creating a model reflecting the behaviour of tested structures may follow.

In further parametric studies the advantage of using numerical analysis is the most significant in reducing the cost and time needed for achieving progress in research of such a structure.

5.1 FEA and meshed model

Finite elements analysis (FEA) software has been successfully used in predicting the behaviour of structures over few decades. Modern FEA software features methods for automatic control and incorporating the last degree of improvements in mathematical and numerical models [19]. In the background of ANSYS FEA software computations is Finite Elements Method (FEM), which discretize mathematical model into finite elements, then the discretized equations are solved and the results are analysed. To obtain reasonable solutions for structural analysis, which contains also the matter of this thesis, is needed to pay attention to setting the basic characteristics of structure like: material characteristics, density of a mesh, boundary conditions and interpretation of solutions [12].

The main advantage of ANSYS compared to other softwares using FEM is in using different forms of elements for mesh which covers the behaviour of modelled structure more realistic [12]. Few examples of elements used by ANSYS are shown below.

SOLID185

Element SOLID185 is one of the elements used to model glass pane. It is a 3D element with eight nodes. Each node has three degrees of freedom – translation in x, y and z direction [20].

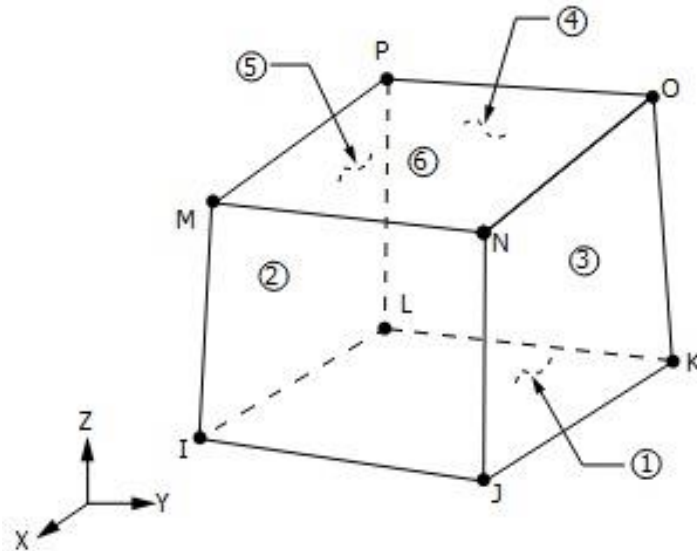


Figure 5.1: Element SOLID185 [20]

SOLID95

SOLID95 is a higher order 3D element. It has twenty nodes with three degrees of freedom (translations in all three directions) [20].

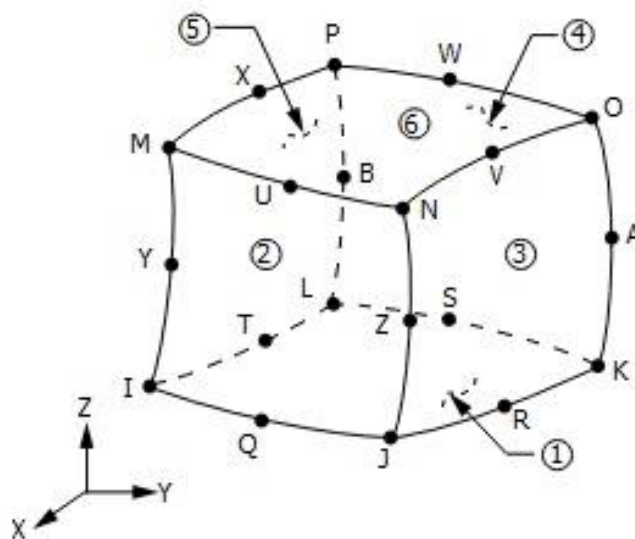


Figure 5.2: Element SOLID95 [20]

5.2 Numerical model

A three-dimensional model was created which will represent tested beams. To define geometry of same dimensions as specimens, the SpaceClaim interface was used. The shape of component allowed us to model only half of beam and use the symmetry of tested specimens. This approach brought time savings and less requirements for hardware during computation as personal laptop was used for gaining results of stress distribution on modelled structure.

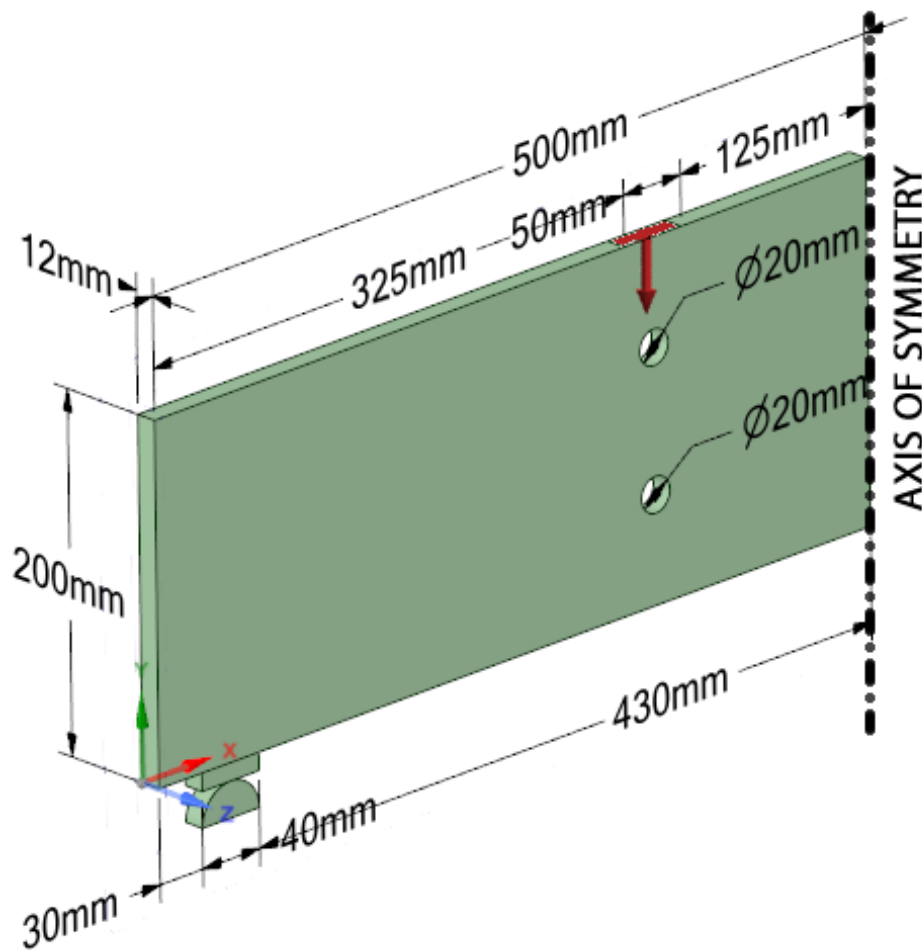


Figure 5.3: Geometry of used model

5.2.1 Input data

The creation of the model with exactly the same behaviour as tested specimen had, or at least with the one which resembles very much to one obtained during the tests, is necessary for providing a parametric study. During tests, force and vertical deflection were measured. From those values stiffness of each specimen was estimated as described in *Chapter 4.6*.

Stiffness is property of whole structure depending on its cross-section area, length and modulus of elasticity. Elastic materials like glass can be defined in ANSYS software by Young's modulus and Poisson's ration, thus those material characteristics were input with respect to average stiffness gained from the experiments and to properties of glass mentioned in *Table 2.1*.

Plastic washer of polyamide, through which the force was applied to glass beam was replaced in model due to its high level of anizotropy and unclear material properties. The support composed of 2 pieces shown in Figure 5.3 consist of Structural steel material and for the beam itself the heat-strengthened glass material was used. The exact values of material properties used for model are obvious from the following tables.

	A	B	C	D	E
1	Property	Value	Unit		
2	Material Field Variables	Table			
3	Density	2500	kg m ⁻³		
4	Isotropic Elasticity				
5	Derive from	Young's Modulu...			
6	Young's Modulus	56500	MPa		
7	Poisson's Ratio	0,23			
8	Bulk Modulus	3,4877E+10	Pa		
9	Shear Modulus	2,2967E+10	Pa		

Table 5.1: Material properties of Heat-strengthened glass used for model

	A	B	C	D	E
1	Property	Value	Unit		
2	Material Field Variables	Table			
3	Density	7850	kg m ⁻³		
4	Isotropic Secant Coefficient of Thermal Expansion				
6	Isotropic Elasticity				
7	Derive from	Young's Modulu...			
8	Young's Modulus	2E+11	Pa		
9	Poisson's Ratio	0,3			
10	Bulk Modulus	1,6667E+11	Pa		
11	Shear Modulus	7,6923E+10	Pa		
12	Alternating Stress Mean Stress	Tabular			
16	Strain-Life Parameters				
24	Tensile Yield Strength	2,5E+08	Pa		
25	Compressive Yield Strength	2,5E+08	Pa		
26	Tensile Ultimate Strength	4,6E+08	Pa		

Table 5.2: Material properties of Structural steel used for model

FORCE

In model the load is applied through area marked in *Figure 5.3* which represents the plastic washer from polyamide used during experiments.

SUPPORT

For support 2 components were created. Prism is supported by cylinder and both are bonded to glass beam model. This layout allows rotation of the beam around support and leads to significant reduce in peak stresses.

5.2.2 The mesh

As student licensed version of software ANSYS Workbench was used, there is a limitation in number of nodes used in one model. This limit is set to maximum of 32 000 nodes, thus using the symmetry was helpful in getting finer mesh compared to one which would be created if full length of the beam was modelled. Generating the mesh and computation were run in the Mechanical interface. Element's maximum size was set to 7,5 mm. To gain optimal density of mesh, tools for fining the mesh locally like "Face sizing" and "Edge sizing" around openings were applied. In total 30 117 nodes and 5 740 elements were used.

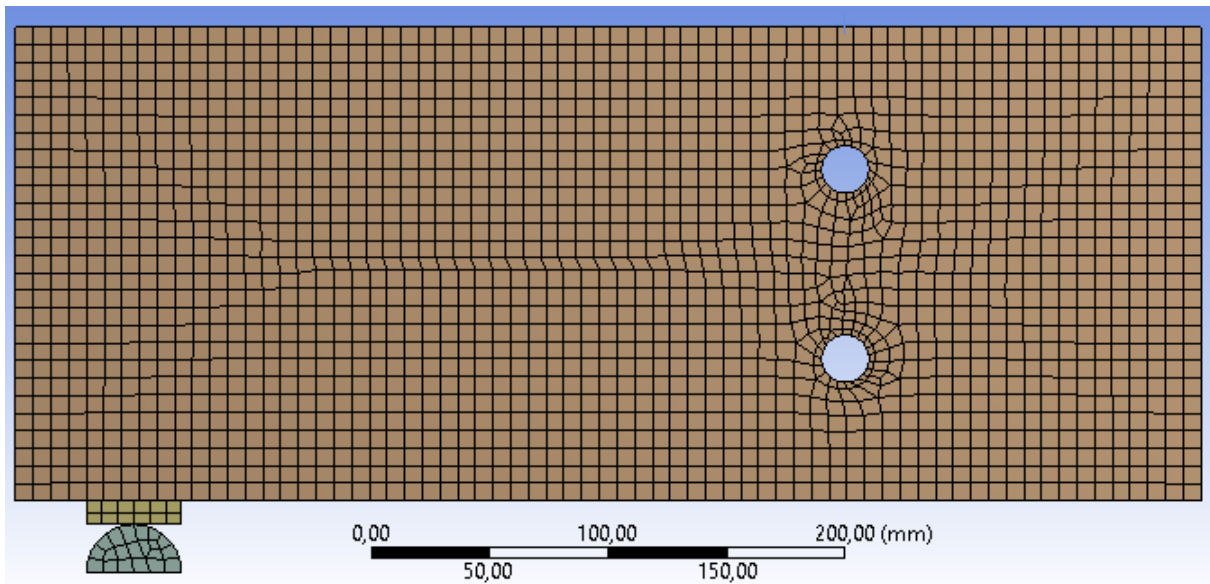


Figure 5.4: Finite elements mesh generated in the Mechanical interface

5.2.3 Boundary conditions and load

As the symmetry of model was used, thus static scheme of structure was changed as well. Changes provided in scheme do not influence the results, meaning that if whole length of beam would be modelled, results would be similar. As mentioned above, the change allowed us using more dense mesh. The force applied to the model corresponds to average value at breakage measured during the experiments. The applied load is 17,92 kN. The scheme of supports used for model are obvious from the figure below.

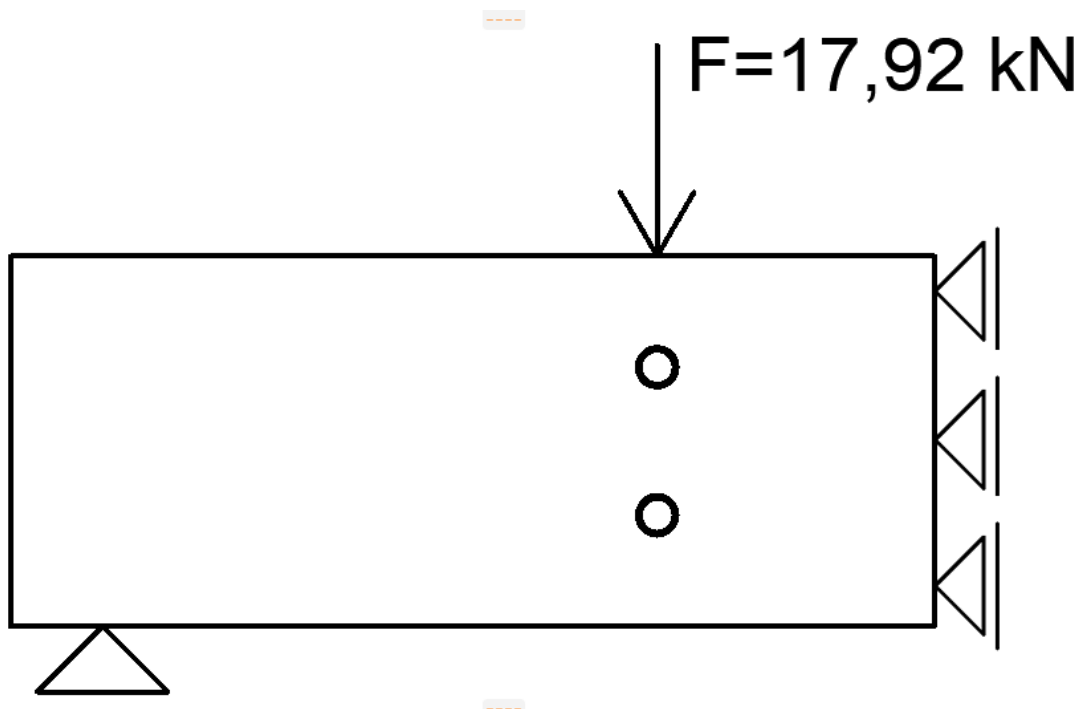


Figure 5.5: Static scheme of used model

5.2.4 Results

Numerical model reached at the loading by force $F = 17,92$ kN which is half of the total average force applied by crosshead in experiments, maximum vertical deflection of 1,155 mm. Estimated stiffness as well as deflection corresponds with the average values stated in *Table 4.1*. Thus, this signifies that the behaviour of modelled structure resembles the behaviour of tested specimens and numerical model was created correctly. The distribution of deflection in direction of y – axis (vertical deflection) with maximum deflection marked, is shown in the *Figure 5.6*.

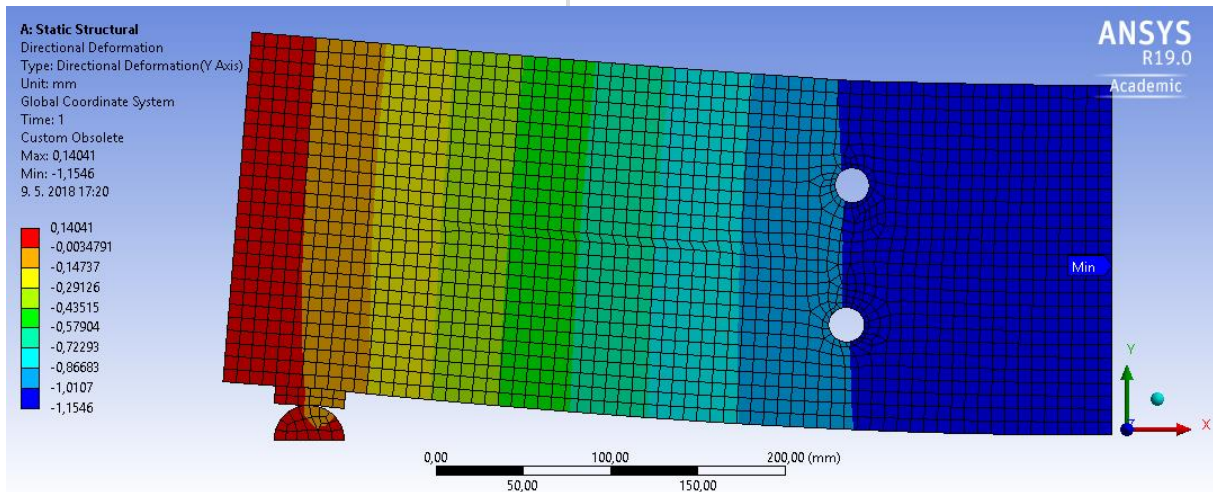
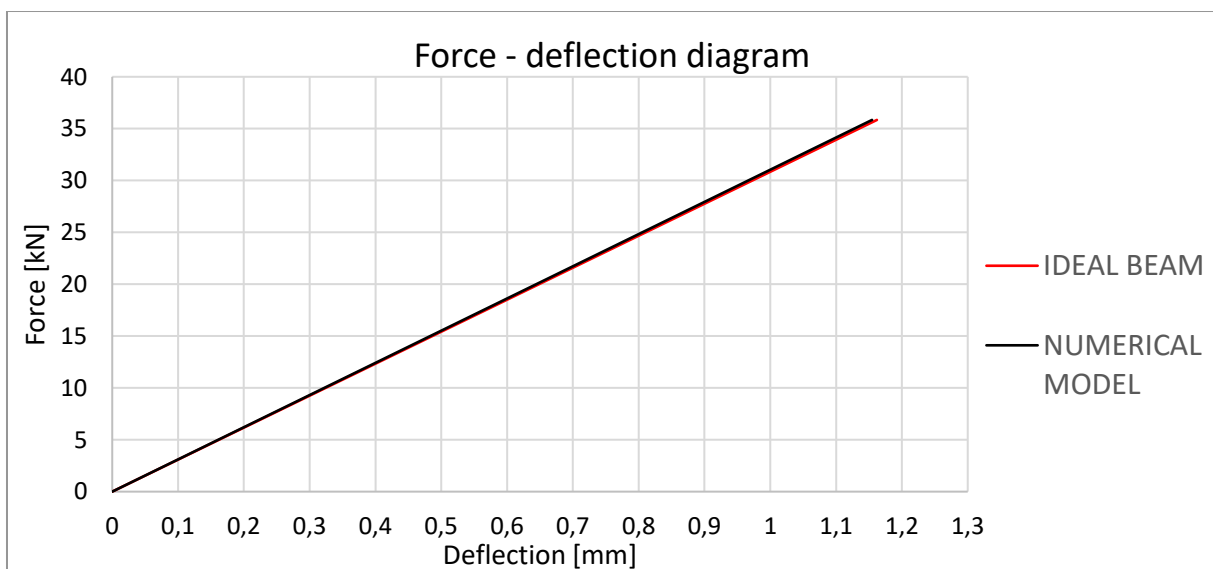


Figure 5.6: Vertical deflection of numerical model

Calculated stiffness of numerical model is $K = 31,041 \text{ kN/mm}$ which is almost identical to average stiffness of tested specimens, which is $K = 31,067 \text{ kN/mm}$. As glass is elastic material, the force – deflection diagram of tested beam in ideal conditions should be linear as shown in the graph below. Conditions in numerical analysis were simulated as ideal, thus this allows the comparison of ideal beam which stiffness was estimated with regard to average values measured during experiments and numerical model. The both presented lines are linear and are almost identical, which underline the previous statement of correctness of the used method and numerical model itself.



Graph 5.1: Comparison of ideal beam and numerical model

Stress distribution on modelled beam is shown in *Figure 5.7*, which corresponds to the stresses measured in experiments at the close proximity of points where strain gauges were placed (*Figure 4.12*). Due to simplified modelling of support are peak stresses noticeable in the area of supporting components, which significantly overcome the load bearing capacity of heat – strengthened glass. Also peak stresses occur in the area close to the surface where the force was applied to. The stresses around mentioned areas do not reflect the real behaviour of tested beams and are not taken into account. Thus, the maximum stress counted in appears at the bottom edge of lower opening, at the point, where initial crack happened during the tests.

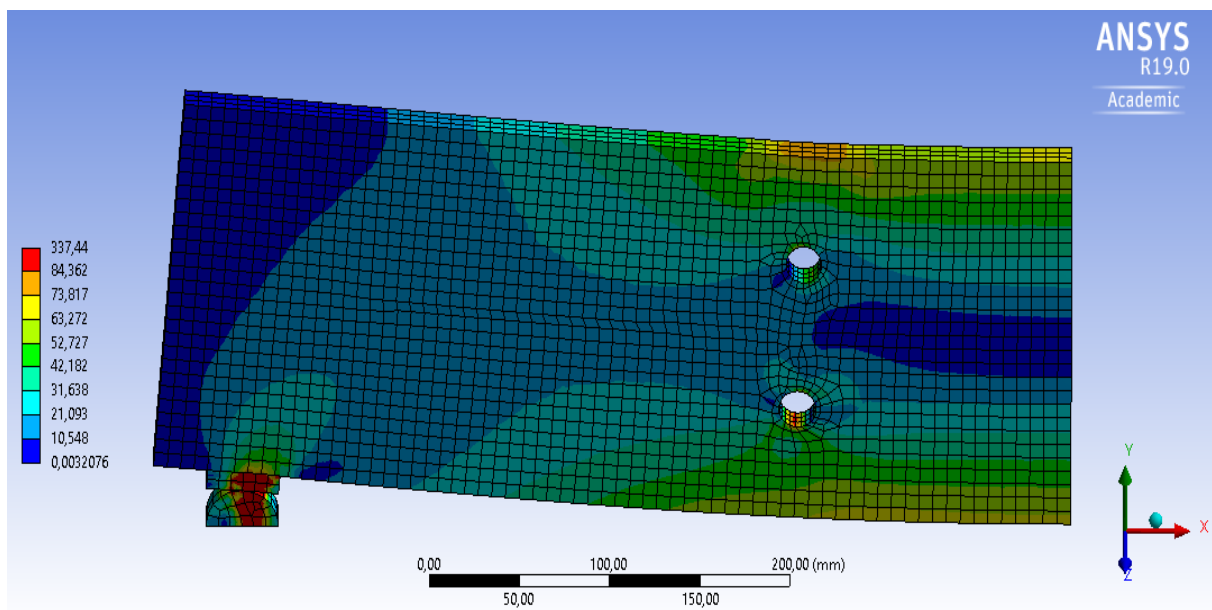


Figure 5.7: Stress distribution on the modelled beam in MPa

Marked maximum stress in *Figure 5.8* reaches 90,129 MPa. Characteristic bending strength of heat–strengthened glass according to EN 1863: Glass in building - Heat strengthened soda lime silicate glass is 70 MPa. Same behaviour, where tested specimen reaches at brittle failure stress about 30% higher than its characteristic bending strength, in this case 28,5%, was recorded during different experiments involving tempered or heat-strengthened glass held at the faculty.

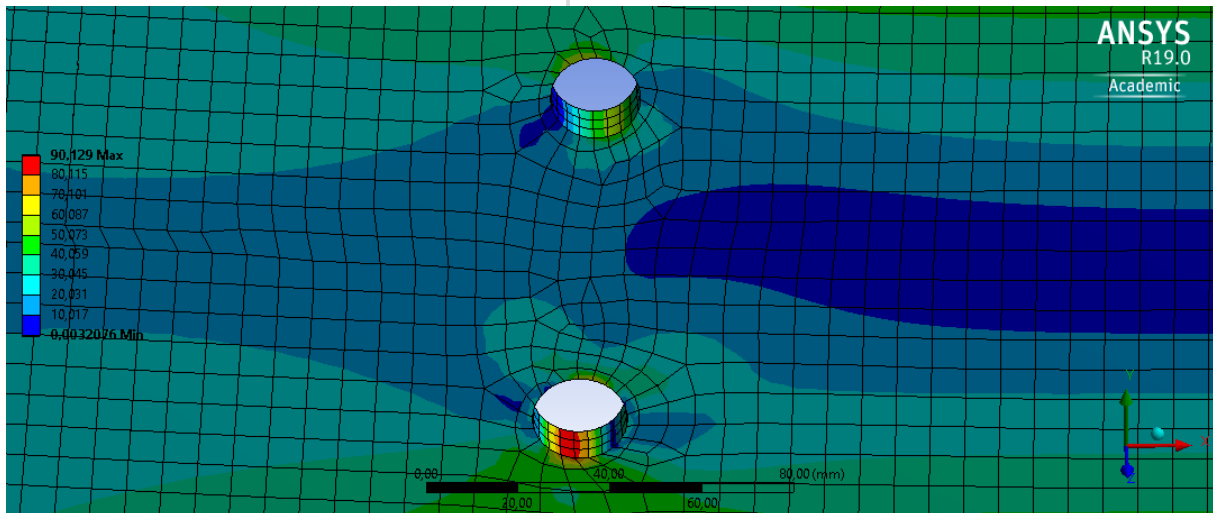


Figure 5.8: Maximum stress at the edge of lower opening in MPa

5.3 Parametric study

Validated numerical model with the same material characteristics and with unchanged way of support and load application, will be used in parametric study. Essential to this parametric study is to monitor changes in stress distribution around the openings, while using:

- different position of holes with diameter 20 mm according to the edges of the beam
- different radius of holes

5.3.1 Variable position

The distance between the holes was symmetrically changed with respect to horizontal axis of symmetry of the beam. The values of the axial vertical distance between the holes, as well as distance between the edge of the hole and longer edge of the beam used for parametric study are shown in *Table 5.3*. In mentioned table the axial distance is marked by shortcut “a” and the edge to edge distance is represented by “b”. Stresses shown in the table were measured at the bottom edge of the lower opening. Although, maximal stresses presented for the axial distance 30, 40, and 60 mm were not the maximum stresses reached on the beam. Starting with the axial distance 80 mm, all maximum stresses occurred at the bottom of edge of lower opening.

a [mm]	30	40	60	80	100	120	140	150	155	160	170
b [mm]	75	70	60	50	40	30	20	15	12,5	10	5
Max σ [Mpa]	48,24	52,46	69,33	90,13	103,04	125,79	159,14	168,07	191,84	191,37	284,67

Table 5.3: Input and output parametric quantities for variable position of opening

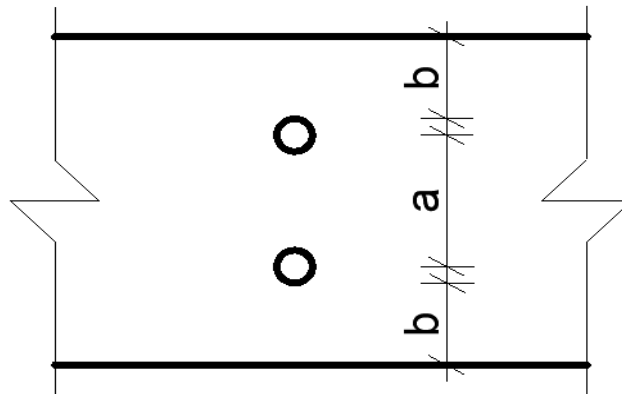
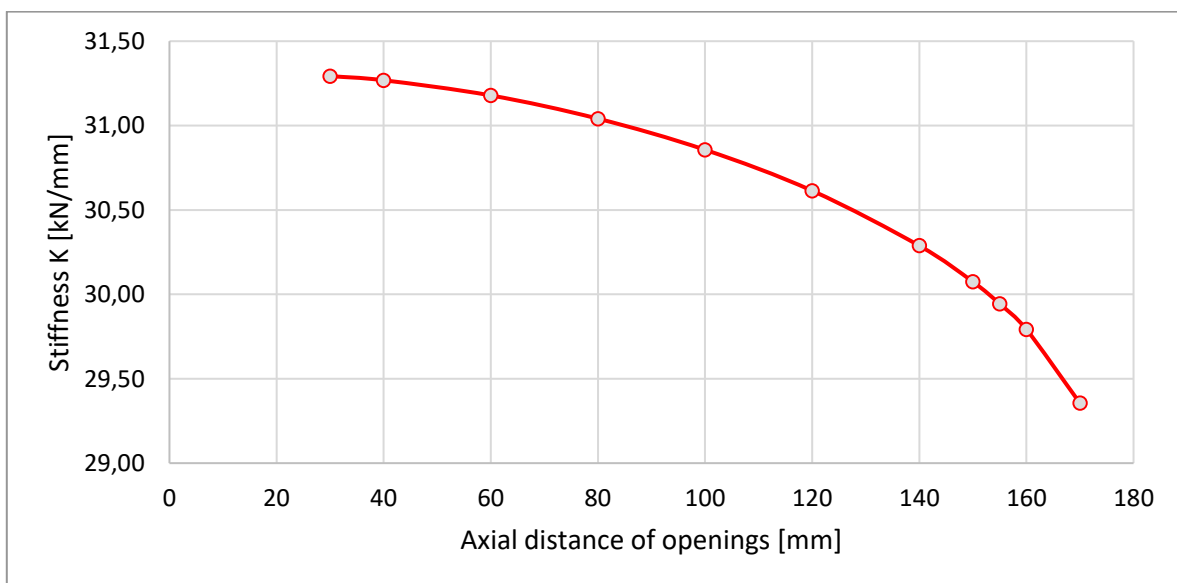


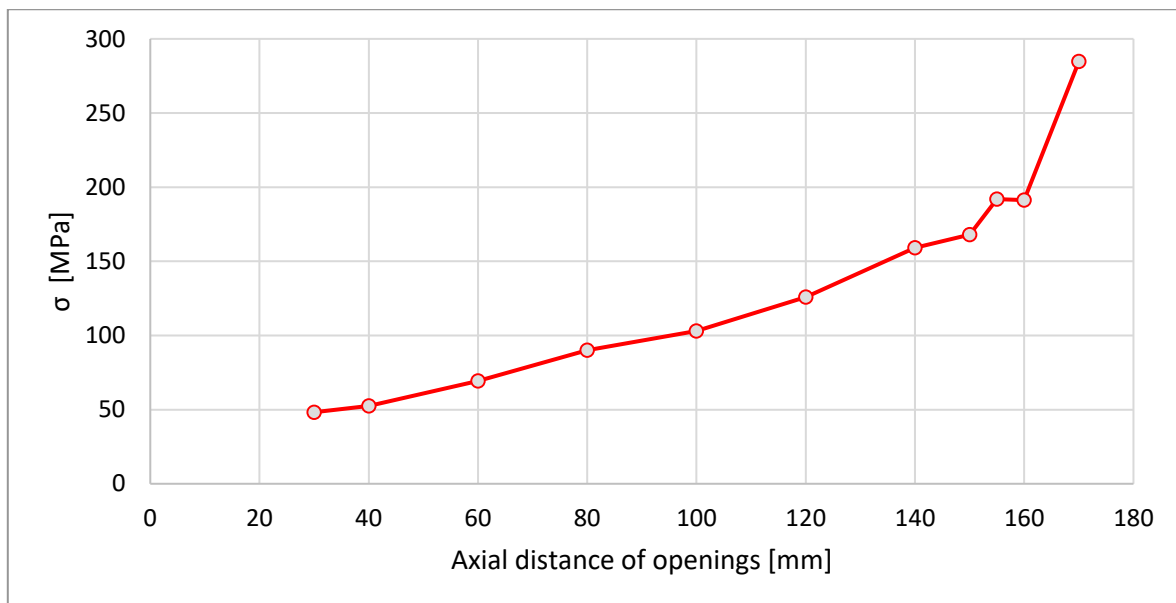
Figure 5.9: Distances "a" and "b"

Even the mass of glass remained unchanged for this part of parametric study, the decrease in stiffness of the beam was recorded and is shown in *Graph 5.2*. The closer the openings were to the edge of beam, the lower stiffness was. The decrease in stiffness is quadratic, as it depends on the moment of inertia. While the difference in stiffness when the axial distances was 30 mm and when it was 140 mm (20 mm from edge of hole to edge of the beam, which is also the diameter of the hole) is 3,3%, the difference in stiffness when the axial distance was 140 mm and when it was 170 mm (5 mm from edge of hole to edge of the beam) is 3,1%.



Graph 5.2: Correlation between the axial distance between the openings and stiffness

Not only stiffness changes with different position of openings but also maximum recorded stress in close proximity of openings rises significantly as the holes are drilled closer to the edge of beam. In bending caused by 4 point flexural test the bending stress is zero at the beam's neutral axis, which is identical with the horizontal axis of symmetry of presented beam. The bending stress increases linearly away from the neutral axis until the maximum values at the extreme fibers at the top and bottom of the beam. Thus, linear change in stress was expected for every axial distance chosen for this parametric study. But as shown in *Graph 5.3*, significant increase which interrupts the linear character of increment of the stress develops after reaching the axial distance of holes of 150 mm (15 mm from the edge of hole to edge of beam). The wavy character of the diagram between axial distances of 30 mm and 150 mm is presumably caused by the limitation in mesh density.



Graph 5.3: Correlation between the axial distance between the openings and maximum principal stress at the edge of hole

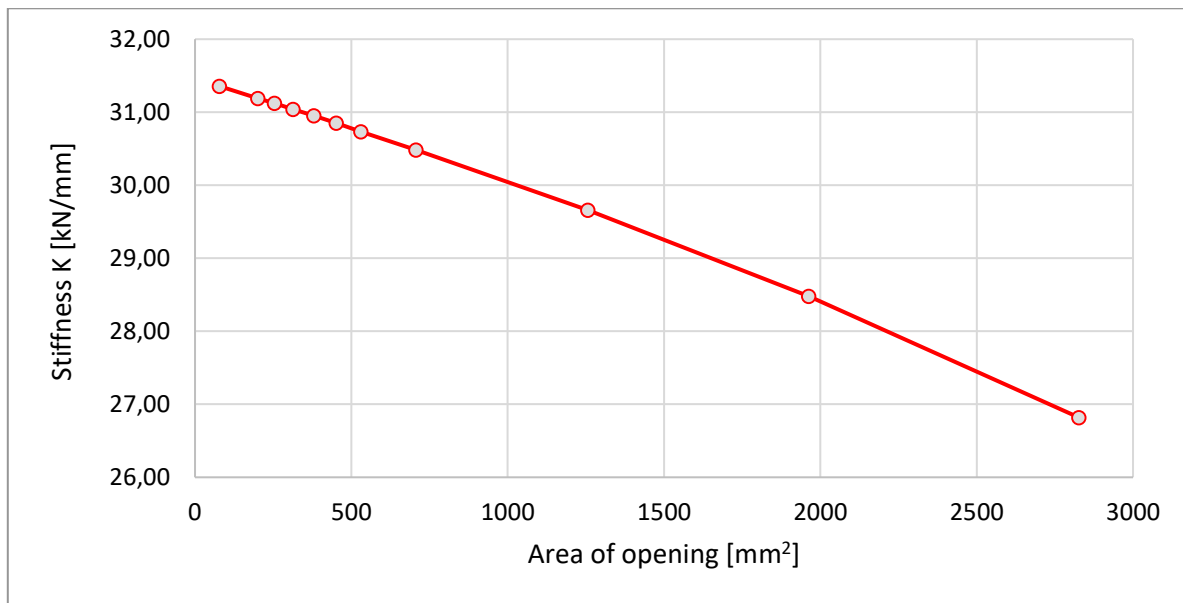
5.3.2 Variable radius

The radiuses used for this parametric study are shown in *Table 5.4* together with maximum stress recorded at the bottom edge of lower opening and stiffness of modelled beam. Radiuses of both openings were changed simultaneously and centre of rotation of holes remained unchanged. Horizontal distance of the holes' axis from the left edge of beam is 350 mm, the vertical axial distance between holes is 80 mm and the vertical distance from the bottom edge of beam to axis of lower opening is 60 mm.

r [mm]	5	8	9	10	11	12	13	15	20	25	30
Max σ [Mpa]	74,73	88,01	86,92	90,13	83,89	88,71	92,44	97,24	108,14	122,52	143,51
K [kN/mm]	31,36	31,19	31,12	31,04	30,95	30,85	30,73	30,48	29,66	28,48	26,82

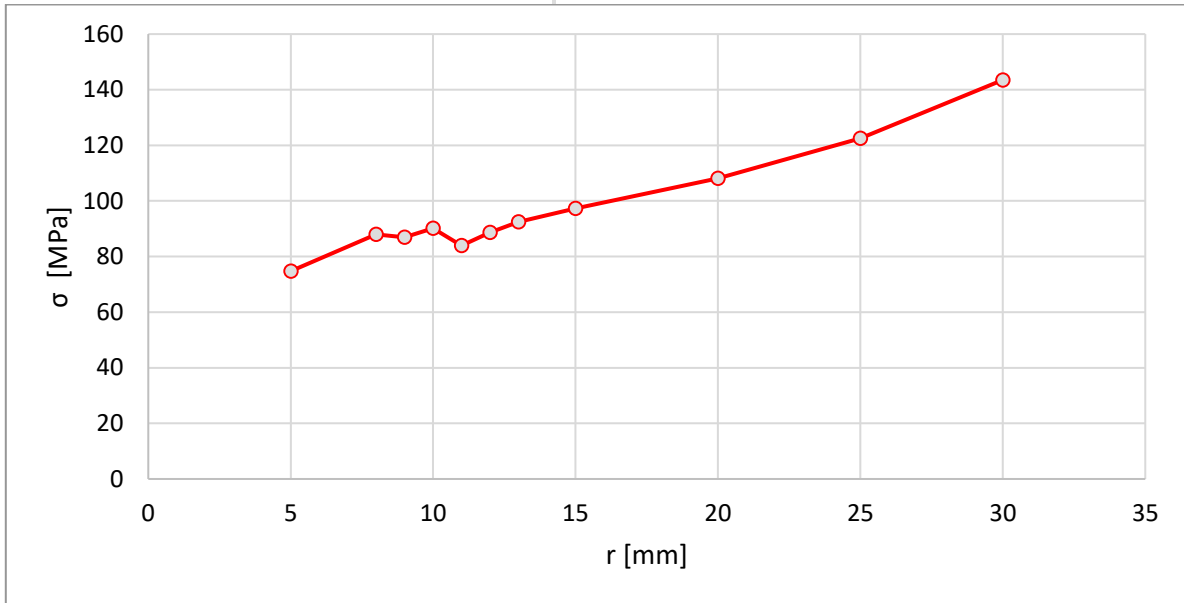
Table 5.4: Input and output parametric quantities for variable radius of opening

The decrease in stiffness shown in the diagram below is obvious. Stiffness of modelled beam changes linearly as mass of glass is reduced by increasing the area of one opening. Recorded behaviour was expected.



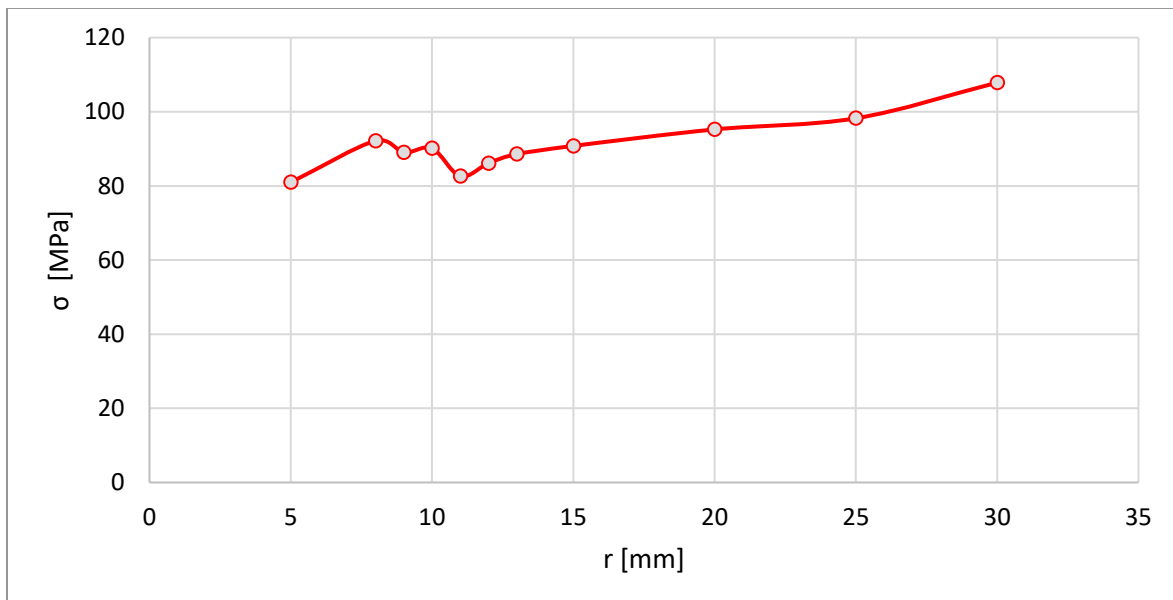
Graph 5.4: Correlation between the area of the opening and stiffness

Influence of radius of the openings on stress distribution is shown in the diagram below. In presented *Graph 5.5* output quantity is stress at the bottom edge of lower opening. As centre of rotation of openings remained in the same position for all used diameters, the effect of increase respectively decrease in stress caused by linear distribution of stress alongside the height of the beam starting with zero at neutral axis and reaching its maximum at the edges is not involved in the following diagram.



Graph 5.5: Correlation between the radius of the opening and maximum principal stress at the edge of hole

For comparison, Graph 5.6 contents measured maximum stress at the edge of hole with the influence of distance from neutral axis counted in. In other words, the real and only effect of different radius of hole on stress distribution in its close proximity is shown. The minimal stress of 82,60 MPa was recorded for radius of 11 mm. For radiuses from 8 mm to 20 mm the stress varies in range of 13 MPa.



Graph 5.6: Correlation between the radius of the opening and maximum principal stress at the edge of hole after subtracting the effect of different edge position alongside the height of beam

6 Conclusion

The research part of presented thesis involves experimental analysis and numerical analysis with parametric study.

Experiments consisted of 3 specimens made out of heat-strengthened glass which were tested in four point flexural test. When the strength of specimens was exceeded, brittle failure characteristic for glass structures appeared immediately. Then, the crack pattern and shards were studied carefully and the bottom edge of lower opening (*Figure 4.19*) was identified as the point of initiation of crack which spread promptly across the whole beam. The average stiffness of all 3 specimens was $K = 31,067$ kN/mm and maximum average vertical deflection was $\delta = 1,162$ mm.

In following numerical analysis using software ANSYS Workbench the Young's modulus $E = 56,5$ GPa was estimated with respect to the applied load and maximum vertical deflection reached during experiments. Mentioned numerical analysis revealed the stress distribution around the openings.

Parametric study provided the data which were compared to *Chapter 2.6* with stated suggested diameters of openings and their distances from edges of glass panes, which glass beams are part of. For parametric study where different axial distance between the openings were used with unchanged diameter, the change of stiffness was quadratic. It was decreasing as the axial distance of openings was increasing due to change of the moment of inertia of the beam. Suggested edge distance for designers stated in *Chapter 2.6* is $A \geq 2S$, where A is hole edge to beam edge distance and S is thickness of glass pane. But dramatic changes in stress occurred in $A = 0.75S$ distance. Although, the stress was changing almost linearly as shown in *Graph 5.3* from the axial distance of 30 mm until 150 mm, which is 15 mm from edge to edge.

The minimal distance between the edges of holes, during this parametric study, was set to 10 mm, but no non-linear change in stress or peak stresses caused by the close proximity of holes were recorded. Due to low stress in the area where openings were the closest, the parametric study with similar input conditions should be held, but in an area of structure with bigger stresses compared to one in this parametric study

As suggested by [1] and [2] diameter of a hole in the in-plane loaded glass pane should fulfil the formula $D \geq S$, where D is diameter and S is thickness of glass pane. But from the perspective of stress quantity, opening of radius 11 mm (diameter 22 mm) showed as the most effective for the beam of height of 200 mm, length 1 000 mm and thickness of 12 mm, as shown in Chapter 5.3.2. The parametric study not only confirms proposed formula, moreover new condition $D \approx 2S$ could be deduced for the same beams as used in this parametric study in order to reach economic design with respect to maximum stress, but further research must be provided.

6.1 Future extensions

To continue in unrevealing the behaviour of glass, the following researches should be carried out to enrich the knowledge of strength and stability of glass beams:

- Testing glass panes with openings of different thickness and diameters of hole
 - to test if similar stress values and its distribution will be observed when $D \approx 2S$
- Relevancy of hole diameter and its distance to edge of glass beam on stress distribution
- Stress distribution in glass pane during drilling of opening
 - as significant stress may be introduced by a drill to glass pane which may lead to its cracking before applying into construction this study should be held
- Use of variable shape of openings
 - as new technology of drilling like CNC machines is used more and more nowadays, different shapes of holes like elliptical may be cut off

7 Bibliography

1. WURM, Jan. *Glass structures: design and construction of self-supporting skins*. Basel: Birkhäuser, c2007. ISBN 978-3-7643-7607-9.
2. O'REGAN, Chris and col., *Structural use of glass in buildings (Second edition)*. London: *The Institution of Structural Engineers*, c2015. ISBN 978-1-906335-25-0.
3. WALD, František, Josef MACHÁČEK, Martina ELIÁŠOVÁ, et al. *Novinky v navrhování ocelových a dřevěných konstrukcí se zaměřením na skleněné konstrukce*. Praha: České vysoké učení technické v Praze, 2015. ISBN 978-80-01-05780-3.
4. ELIÁŠOVÁ, Martina. *Lectures of Glass structures*, Department of Steel and Timber Structures, Faculty of Civil Engineering, CTU in Prague. 2015.
5. LORENZ, Jan. (2016). *Numerical analysis of glass pane. Diplomová práce*.
6. WÄLCHLI, Ernst, KASSNEL-HENNEBERG, Bruno. *A True All-Glass Staircase*. BOS, LOUTER, NIJSSE, VEER (Eds.). *Challenging Glass 3 – Conference on Architectural and Structural Applications of Glass*. IOS Press 2012. ISBN 978-1-61499-061-1-151
7. JIRÁSEK, Jakub, VAVRO, Martin. *Výukové materiály – Sklo*. Institut geologického inženýrství, Hornicko-geologická fakulta, VŠB-TU Ostrava.
<http://geologie.vsb.cz/loziska/suroviny/> [online] (zobrazené 1.4.2017)
Available at:
<http://geologie.vsb.cz/loziska/suroviny/sklo.html>
8. HŘÍBOVÁ, Martina. *SKLÁŘSTVÍ VE 13.-16. STOLETÍ V ZÁPADNÍ A STŘEDNÍ EVROPE*
Available at:
<http://firing.wz.cz/Sklo.htm>
9. VENCL, Radim (2011). *Analýza chování nepředepnutých šroubovaných spojů konstrukcí ze skla*. Dizertačná práce
10. HALDIMANN, Matthias, LUIBLE, Andreas, OVEREND, Mauro. *Structural Use of Glass*, Zürich: ETH Zürich, c2008. ISBN 978-3-85748-119-2.
11. UNGUREANU, Viorel. *Advanced design of glass structures, Lecture 3 – Laminated glass and interlayers, European Erasmus Mundus Master Course Sustainable Constructions under Natural Hazards and Catastrophic Events*. 520121-1-2011-1-CZ-ERA MUNDUS-EMMC,
Available at:

http://www.ct.upt.ro/suscos/files/2013-2015/1E05/2E5_Glass_structures_L3_2014_VU.pdf

12. DROZDA, Jiří, HASNÍKOVÁ, Hana, JIRSÁK Václav, MAŠOVÁ, Eva. *Příručka ANSYS Workbench*. Praha: České vysoké učení technické v Praze, Fakulta stavební, Katedra ocelových a dřevěných konstrukcí. 2012. ISBN 978-80-01-05175-7
13. ANSYS Inc. *ANSYS Workbench User's guide*. 2009
14. WELLER, Bernhard, HÄRTH, Kristina. *Experimental Research on Glass-Polycarbonate Beams. Challenging Glass 2 – Conference on Architectural and Structural Applications of Glass*. TU Delft, The Netherlands 2010. ISBN 978-90-8570-524-6
15. WELLER, Bernhard, MEIER, Anja, WEIMAR, Thorsten. *Glass-Steel Beams as Structural Members of Facades. Challenging Glass 2 – Conference on Architectural and Structural Applications of Glass*. TU Delft, The Netherlands 2010. ISBN 978-90-8570-524-6
16. DIN 18008-3. *Glas im Bauwesen – Bemessungs- und Konstruktionsregeln – Teil 3: Punktförmig gelagerte Verglasungen (Glass in Building – Design and construction rules – Part 3: Point fixed glazing)*. 2013
17. FELDMANN, Markus, KASPER R. and col. *Guidance for European structural design of glass components: support to the implementation, harmonization and further development of the Eurocodes*. Luxembourg: Publications Office for the European Union, 2014. EUR. ISBN 978-92-79-35093-1.
18. Dewetron DEWE-5000 user's guide [online, visited on 10.4.2018]
Available at:
<https://www.dewetron.com/products/chassis/all-in-one-chassis/dewe-5000/>
19. COMSOL Inc., *Finite Element Analysis (FEA) software*
Available at:
<https://www.comsol.com/multiphysics/fea-software>
20. ANSYS Online Manuals realise 5.5
Available at:
<http://www.ansys.stuba.sk/html/realtoc.html>